AD NUMBER

ADB033948

LIMITATION CHANGES

TO:

Approved for public release; distribution is unlimited.

FROM:

Distribution authorized to U.S. Gov't. agencies only; Test and Evaluation; 03 JAN 1979. Other requests shall be referred to Electronic Systems Division Center, Attn: TOFL, Hanscom AFB, MA 01731.

AUTHORITY

ESD ltr, 12 May 1981

Project Report

TT-33

XMQM-105 (Aquila) Mini-RPV Vibration and Flight Dynamics Measurements

C. F. Bruce
W. R. Davis

8 December 1978

Prepared for the Defense Advanced Research Projects Agency
under Electronic Systems Division Contract F19628-78-C-0002 by

Lincoln Laboratory
MASSACHUSETTS INSTITUTE OF TECHNOLOGY
LEXINGTON, MASSACHUSETTS

The work reported in this document was performed at Lincoln Laboratory, a center for research operated by Massachusetts Institute of Technology. This work was sponsored by the Defense Advanced Research Projects Agency under Air Force Contract F19628-78-C-0002 (ARPA Order 2752).

This technical report has been reviewed and is approved for publication.

FOR THE COMMANDER

Raymond L. Loiselle

Raymond L. Loiselle, Lt. Col., USAF
Chief, ESD Lincoln Laboratory Project Office

MASSACHUSETTS INSTITUTE OF TECHNOLOGY

LINCOLN LABORATORY

XMQM-105 (AQUILA) MINI-RPV VIBRATION AND FLIGHT DYNAMICS MEASUREMENTS

C. F. BRUCE
W. R. DAVIS
Group 73

PROJECT REPORT TT-33

8 DECEMBER 1978

LEXINGTON MASSACHUSETTS

ABSTRACT

Vibration, flight dynamics, and vertical gust velocity measurements were performed for the XMQM-105 (Aquila) miniature remotely piloted vehicle. The effects of operating the engine over its range of speeds and the influence of the sensor payload vibration isolators were evaluated using ground test vibration data. The amplitudes and spectra of vibration and flight dynamic accelerations were analyzed for test flights in operational-type patterns. One significant flight dynamic motion observed was a yaw oscillation at a frequency of about 0.6 Hz. To provide a specification for the sensor payload vibration environment, the acceleration spectra were enveloped; and the envelopes were modified to remove the effects of the payload isolators. Acceleration time histories were examined for flight maneuvers and transient events, and the peak loads for these conditions were measured.

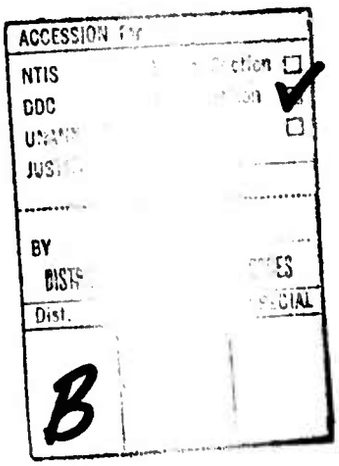

MISSING PAGE
NUMBERS ARE BLANK
AND WERE NOT
FILMED

CONTENTS

LIST OF ILLUSTRATIONS

LIST OF TABLES

INTRODUCTION

The U.S. Army Aviation Research and Development Command (AVRADCOM) has sponsored the development of the miniature remotely piloted vehicle (mini-RPV) XMQM-105 (Aquila) as part of a technology demonstration program. The Aquila was designed and built by Lockheed Missiles and Space Company. Mini-RPV missions include reconnaissance, target acquisition, artillery adjustment, and target designation, all of which are based on data gathered using on-board sensors.

The objective of the MIT Lincoln Laboratory program was to measure and evaluate the vibration and flight dynamic characteristics of the Aquila mini-RPV. Of particular interest were the motions at the location of the on-board sensor package because of the importance of such motions to proper sensor design and operation.

The test program was comprised of two parts, both performed at Ft. Huachuca, Arizona. The ground test portion, performed from 1 to 5 May 1978, was designed to measure the effects of operating at different engine speeds and to determine the influence of the payload vibration isolators.

The second part of the experimental program was the flight portion, which was performed from 9 to 19 June 1978. For the three test flights, aircraft vibration and flight dynamic motions were measured during flight patterns selected to represent those anticipated in operational missions. Measurements were also made of the atmospheric gust environment through which the aircraft flew.

TEST EQUIPMENT

Aircraft Physical Description

The Aquila mini-RPV has an all-wing configuration with a wing span of 3.8 m, wing area of 2.95 m^2, length of 1.9 m, and gross takeoff weight of 65 kg. The maximum range is 300 km, the ceiling is 6 km, and the flight duration is 3.4 hrs. The single-cylinder, two-stroke engine develops 8.7 kw (11.7 hp), which provides for cruising speeds up to 40 m/s. The two-bladed, pusher propeller is surrounded by a cylindrical duct or shroud.

The Aquila airframe structure is made primarily of kevlar and fiberglass, with styrofoam used as the core for the propeller shroud. Three servo actuators are used in the flight control system, one for the engine throttle and two for the elevon control surfaces. A sketch of the aircraft is shown in Figure 1.

Two different aircraft were used during the ground and flight testing. All testing except for the final flight was performed with aircraft S/N 014, and the last flight test was performed with S/N 019.

Guidance and Control

The aircraft guidance was performed from the ground station, which contained a tracking antenna, consoles for the aircraft and sensor operators, a computer, a video monitor and recorder, a navigation plotter, a transmitter, and a receiver. The computer provided guidance between way points whose sequence, altitudes, and airspeeds were programmed prior to flight. The autopilot on board the mini-RPV controlled the aircraft attitude during flight.

Launch and Recovery

The Aquila was launched with a truck-mounted, pneumatic catapult. The catapult travel was about 6.1 m in length, and it provided a launch speed of about 23 m/s.

Prior to the recovery approach, a spring-loaded, hinged framework was deployed to protect the payload sensor and dome. A rectangular, fabric drag brake, attached to the payload protector, was employed to maintain a reduced recovery approach speed.

The recovery system consisted of two net-like sets of arrestor lines (one set vertical and the other horizontal) connected to hydraulic energy absorbers. The aircraft was flown into the vertical lines using operator corrections to the guidance commands during the final recovery approach. The vertical lines halted the forward, horizontal motion of the aircraft, which then dropped onto the horizontal lines. The recovery approach speed of the aircraft can range between 19 and 27 m/s.

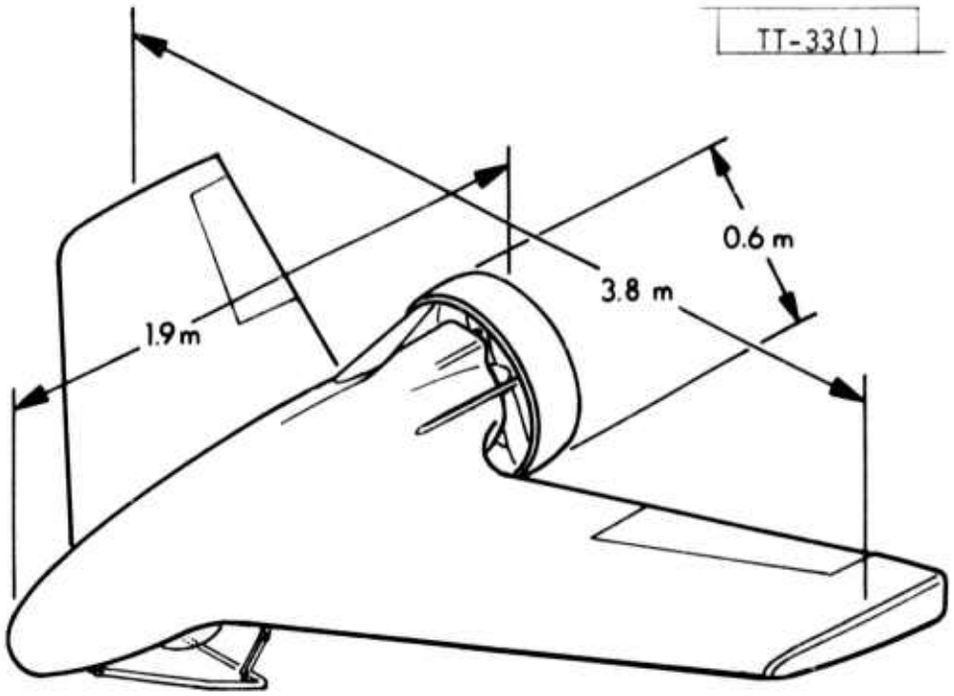

Fig. 1. XMQM-105 (Aquila) mini-RPV.

Ground Test Instrumentation

Three linear servo accelerometers were aligned along the three aircraft axes and rigidly mounted on a special sensor payload plate designed for the vibration and flight dynamics experiments. A diagram of the accelerometer locations is shown in Figure 2. The 2.5 cm thick aluminum plate was located at the payload mounting points, 0.425 m forward of the aircraft center of gravity. A transparent acrylic dome was attached directly to the lower side of the plate, protruding through the bottom of the aircraft fuselage into the airstream. The plate was supported atop four isolators (Barry, Model E22-02-60) which, in turn, were attached to the payload mounting bracket section of the airframe. The total weight of the sensor payload plate during the ground tests was 10.8 kg, including the accelerometers, but less the isolators.

Power supplies for accelerometer input power, filter-amplifiers for signal conditioning, and a multi-channel magnetic tape recorder for data acquisition were connected to the accelerometers as shown in Figure 2 for the ground tests. The range of each accelerometer was ± 20 g's, the sensitivity was .25 V/g, and the frequency range was 0-300 Hz.

Flight Test Instrumentation

An instrumentation package, a gust vane, a video camera, and the autopilot and flight control status transducers were used to study the vibration and flight dynamic motions of the aircraft during flight. Data was transmitted continuously to the ground during the experiments. A diagram of the airborne instrumentation and telemetry equipment is shown in Figure 3.

Instrumentation Package

The six-component accelerometer instrumentation package was developed by Ford Aerospace for a previous AVRADCOM program. The three angular accelerometers were mounted inside the package, and the three piezoresistive linear accelerometers were mounted on a block atop the sensor payload plate as shown in Figure 2. The total weight of the sensor payload plate, including instrumentation package and video camera, was 11.6 kg. The amplitude and frequency ranges for the amplified and filtered accelerometer signals are listed in

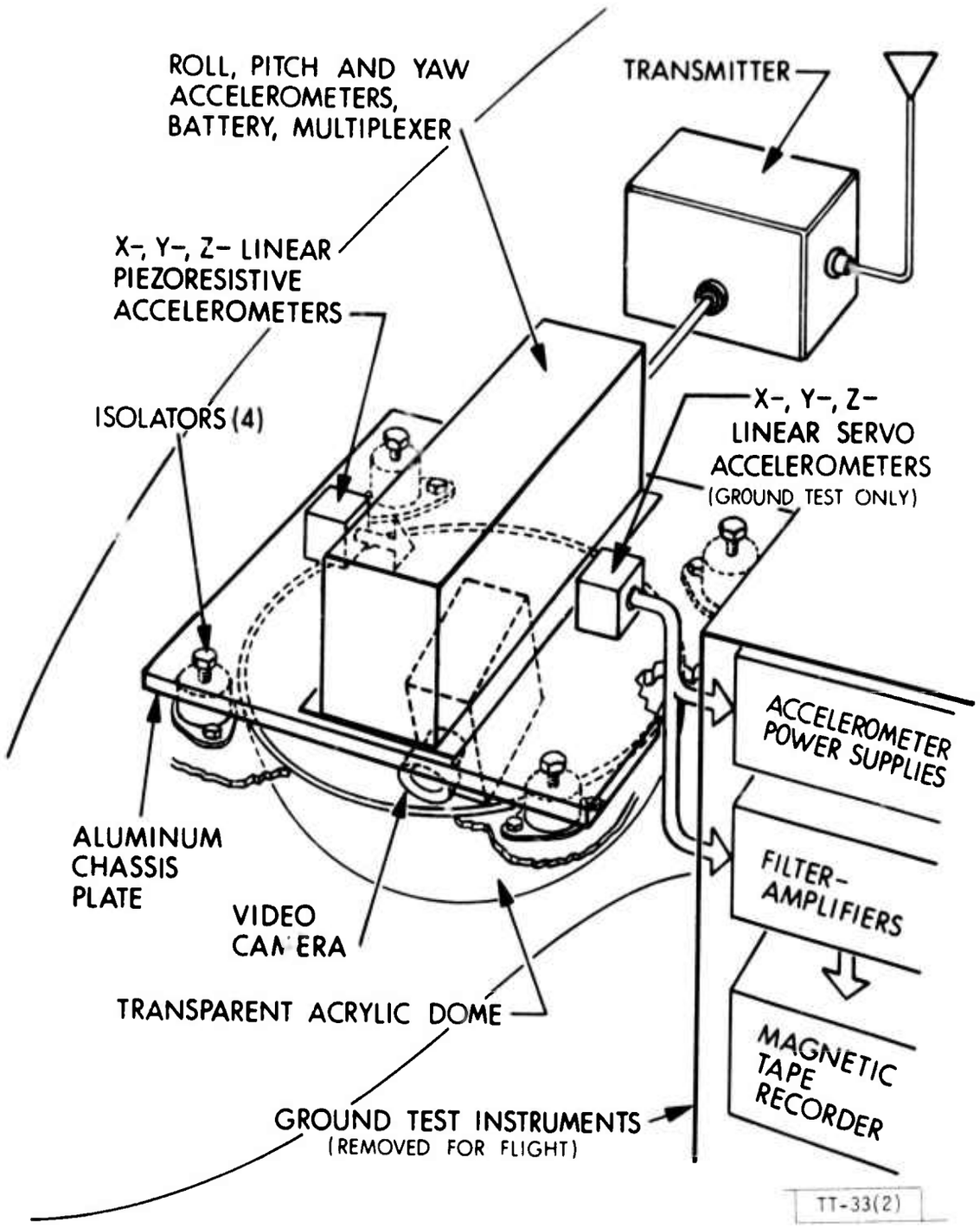

Fig. 2. Aircraft instrumentation.

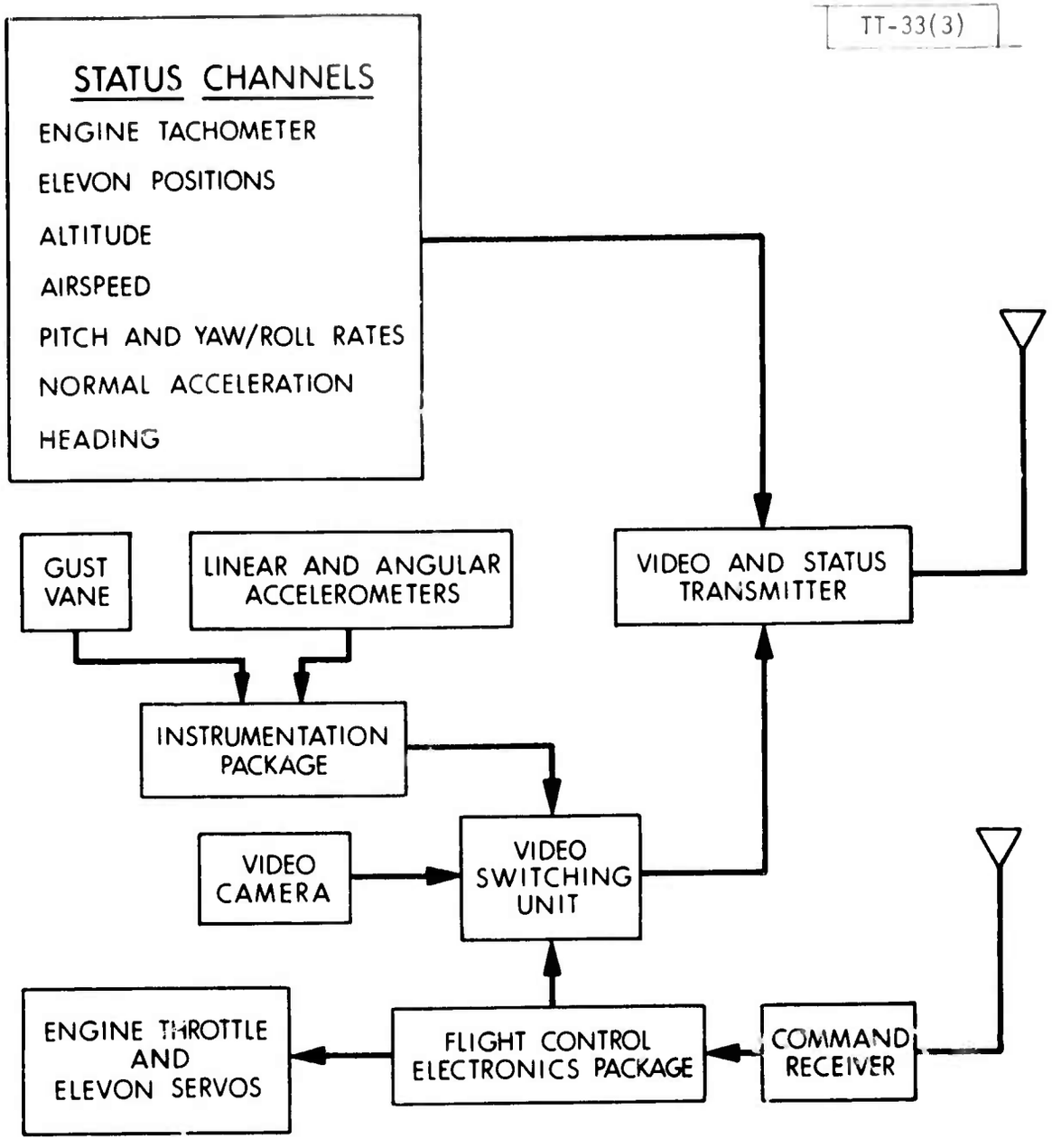

Fig. 3. Airborne instrumentation and telemetry.

Table 1. Two frequency ranges were provided for each linear accelerometer by employing separate low-pass filters and separate telemetry input channels.

The output signal from the package was in a pulse amplitude modulation (PAM) form, with 32 channels sampled at a rate of 750 samples per second per channel and a 50% duty cycle. The three linear accelerometer signals with 0-300 Hz filtering were each connected to two PAM channels with samples equally spaced in time in order to obtain the full frequency range desired. The PAM output signal was switched to replace the video camera signal on the regular Aquila video link when commanded from the ground control station (Figure 3).

A rechargeable battery pack inside the instrumentation package provided ± 24 volts for a nominal operation of one hour. The instrumentation package measured 10.2 x 10.8 x 33 cm, and its weight was 3.6 kg.

Gust Vane

The gust vane was a balsa wood flag attached to a brass shaft, statically balanced with a counterweight, and mounted on a low-torque potentiometer. The potentiometer and signal conditioning electronics were mounted inside a fairing protruding forward of and below the aircraft nose on the end of a fiberglass tube. A photograph of the gust vane and the fairing interior is shown in Figure 4, and a photograph of the installation on the aircraft nose is shown in Figure 5.

The rectangular gust vane had dimensions of 0.16 cm thickness, 2.5 cm width, and 5.8 cm length. The gust vane and potentiometer shaft had a moment of inertia of 6.42 gm cm^2 which yielded natural frequencies (according to formulas in Karam, Reference 1) between 9 and 15 Hz for the range of flight dynamic pressures.

The gust vane was mounted in a horizontal orientation in order to measure the vertical gust velocities of the atmosphere through which the aircraft flew. The vertical gust velocities were determined from the measured vane angles, airspeeds, pitch accelerations, and vertical accelerations according to the relation $w = V\alpha_v - V\theta + \ell\dot{\theta} - \dot{z}$. The symbols are defined as follows: w = vertical gust velocity in meters per second (positive upward), V = aircraft forward airspeed in meters per second, α_v = gust vane angle in radians

TABLE 1

FLIGHT INSTRUMENTATION PACKAGE RANGES

TRANSDUCER	RANGE
X-Linear Accelerometer	± 2.67 g's, 0 - 300 Hz
X-Linear Accelerometer (Low Frequency)	± 2.67 g's, 0 - 6 Hz
Y-Linear Accelerometer	± 2.29 g's, 0 - 300 Hz
Y-Linear Accelerometer (Low Frequency)	± 2.29 g's, 0 - 6 Hz
Z-Linear Accelerometer	± 2.86 g's, 0 - 300 Hz
Z-Linear Accelerometer (Low Frequency)	± 2.86 g's, 0 - 6 Hz
Roll Angular Accelerometer	± 43.4 rad/sec^2, 0 - 27 Hz
Pitch Angular Accelerometer	± 20.0 rad/sec^2, 0 - 36 Hz
Yaw Angular Accelerometer	$\pm$ 4.87 rad/sec^2, 0 - 26 Hz
Gust Vane	$\pm 15^{o}$, 0 - 125 Hz

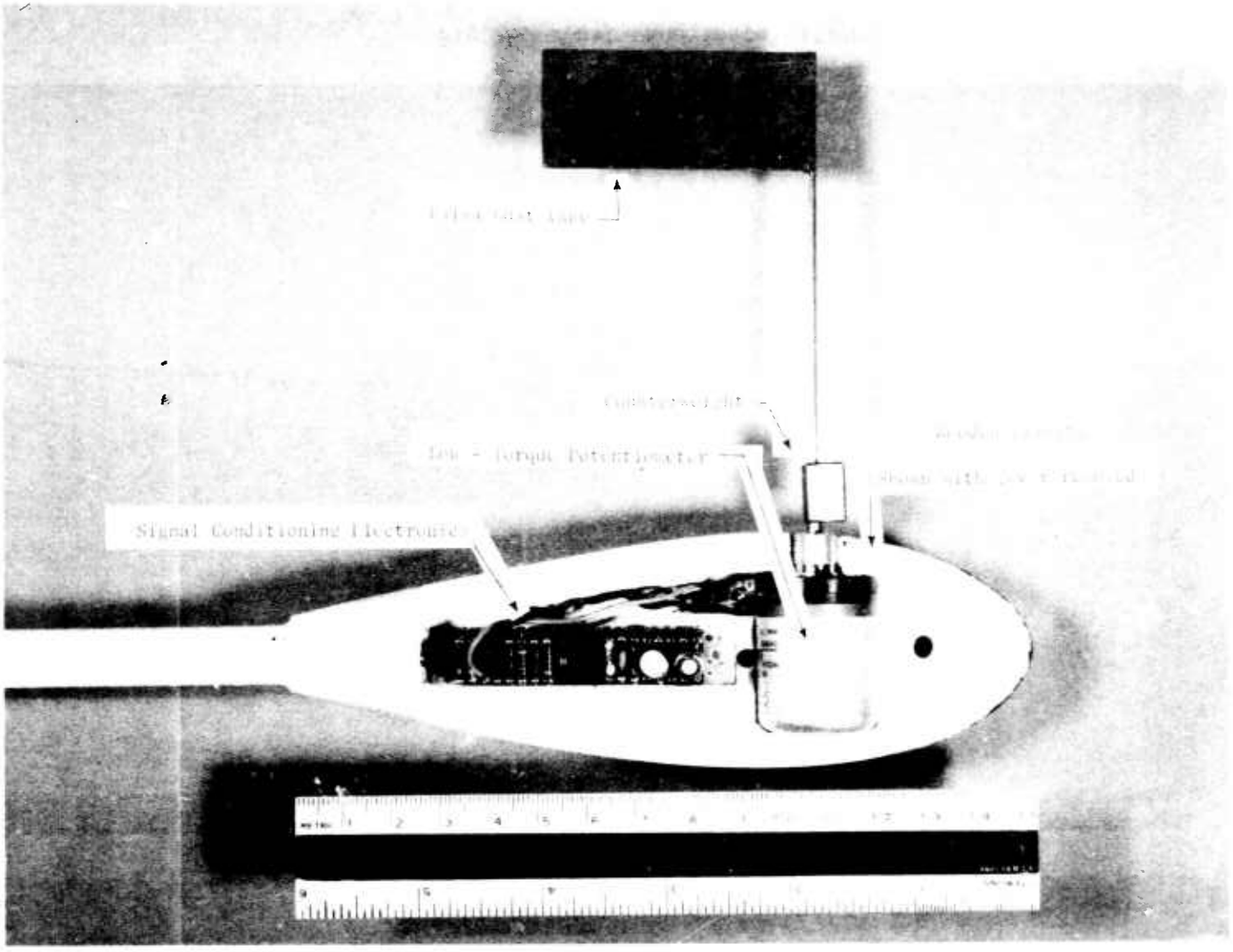

Fig. 4. Gust vane and fairing interior.

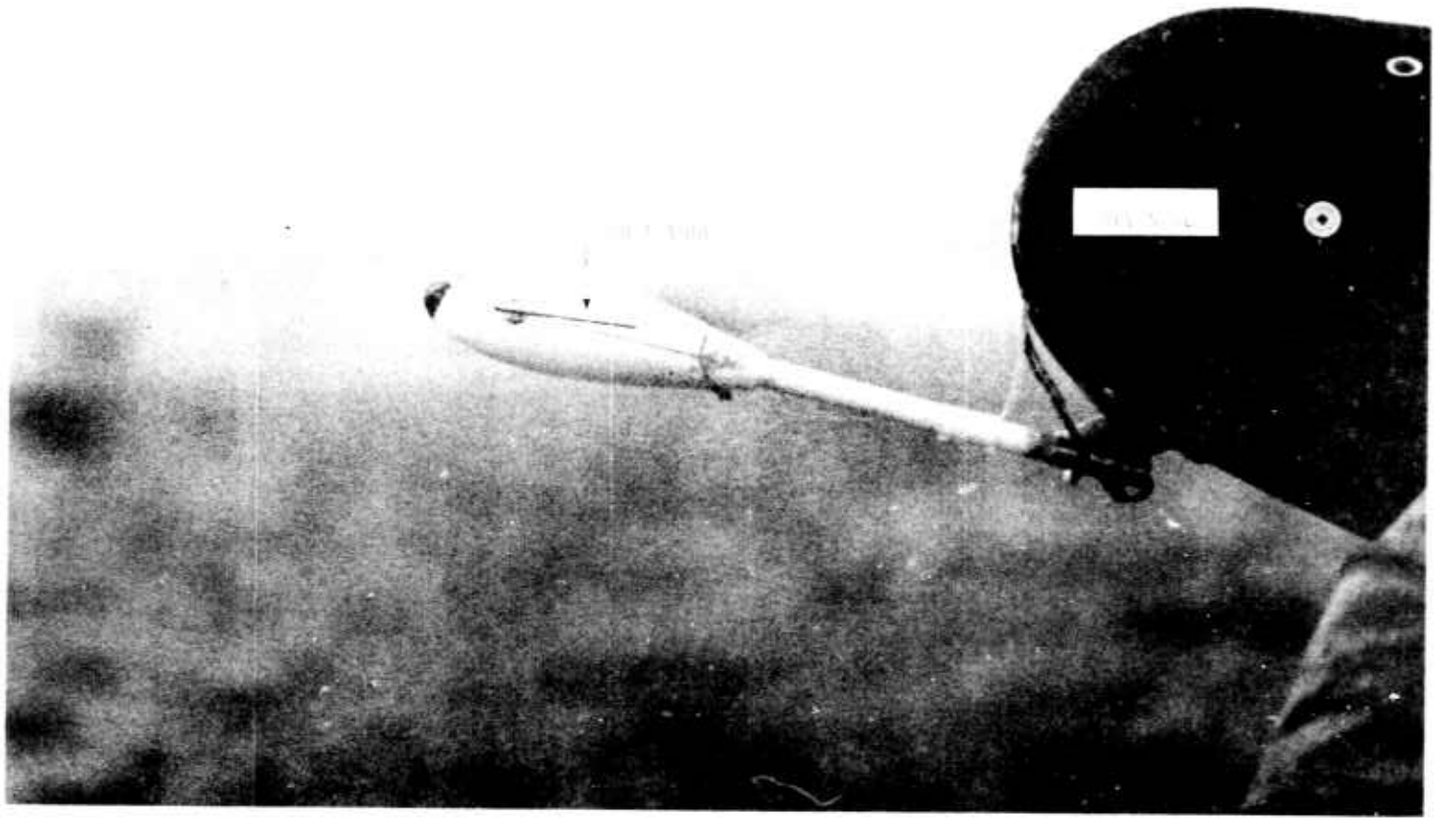

Fig. 5. Gust vane installation.

(positive upward, assumed small), θ = pitch angle in radians (second integral of pitch acceleration, positive upward), ℓ = distance between the gust vane and the location of pitch and vertical accelerometers in meters, $\dot{\theta}$ = pitch rate in radians per second (first integral of pitch acceleration, positive upward), and $\dot{z}$ = vertical velocity in meters per second (first integral of vertical acceleration, positive downward).

Video Camera

A video camera was rigidly attached to the bottom of the sensor payload plate for the flight testing, enclosed by the hemispherical, transparent acrylic dome. It was mounted with a downward inclination to compensate for the trim angle of attack of the aircraft. It provided a view forward of the aircraft on the RPV operator's monitor when the PAM signal from the instrumentation package was not selected.

Status Instrumentation

Data from the vehicle status transducers on the aircraft was encoded on board into a pulse code modulation (PCM) form. Thirty-two words of eight bits each comprised every frame of PCM data, and the PCM frame rate was about 10 frames per second. To determine the aircraft range from the ground control station, the status PCM data stream was synchronized with the command PCM received from the uplink. Then the data was multiplexed with the selected PAM or video signal and transmitted to the ground.

The vehicle status transducers of interest for the flight testing were a tachometer, elevon position transducers, altimeter, an airspeed transducer, a normal accelerometer, a pitch rate gyro, a roll/yaw rate gyro, and a magnetometer for heading.

Ground Station Instrumentation

The status PCM signal and the selected video or PAM signal on the downlink from the aircraft were received by a tracking antenna on the ground control station (GCS). A diagram of the ground station instrumentation is shown in Figure 6. The status PCM data were recorded on a digital magnetic

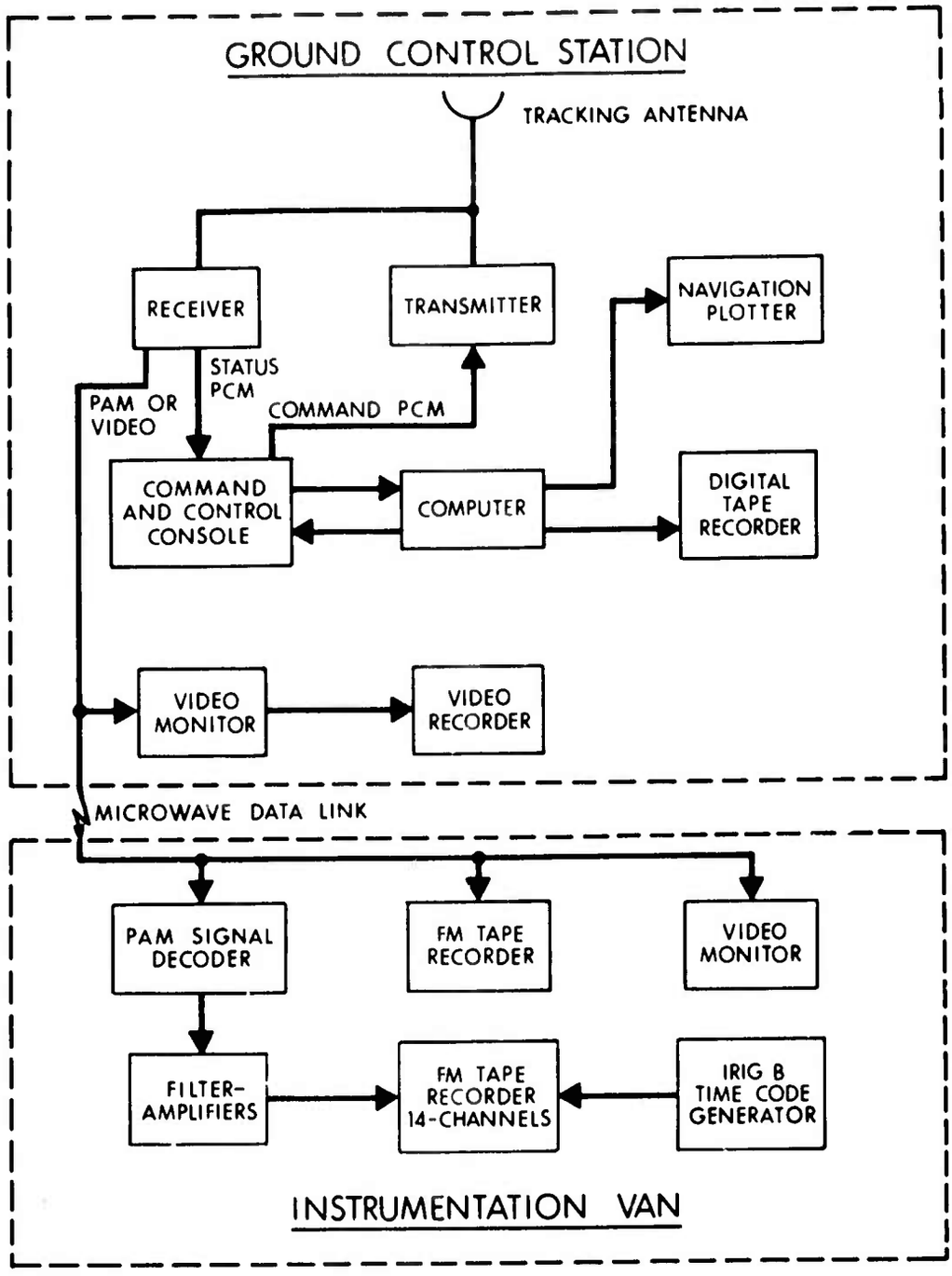

Fig. 6. Ground station instrumentation.

tape recorder in the GCS and selected channels were displayed for the RPV and sensor operators. The video picture from the on-board camera was displayed on video monitors for each operator, and the signal was recorded on a video tape recorder. The programmed and actual flight paths were recorded on a navigation plotter in the GCS.

The selected video or PAM signal from the GCS was connected to an instrumentation van (IV) about 150 m distant through a microwave data link. The video picture was displayed on a monitor in the IV, and the full PAM signal was recorded on a magnetic tape recorder. The PAM signal was also fed into a twelve-channel decoder. The decoded PAM signals were filtered and amplified, as required, and recorded on a fourteen-channel FM magnetic tape recorder. The signal from an IRIG B time code generator was also recorded on the fourteen-channel recorder in the IV.

Meteorological information was provided from the GCS and from the central meteorological observatory at Fort Huachuca. The GCS data included winds for the launch and recovery, and the observatory data included winds aloft and ground-level temperature, pressure, and density altitude.

TEST PROCEDURES

Ground Testing

Ground testing was performed to measure vibrations at the sensor mounting during engine operation, with the aircraft removed from the flight environment. The test data was used to evaluate the influence of the sensor payload vibration isolators and to select the amplifier gains and filtering for the flight instrumentation.

The three linear servo accelerometers were mounted to the sensor payload plate and connected to the power supplies and filter-amplifiers as shown in Figure 2. Each accelerometer, filter-amplifier, and recorder channel was calibrated.

The aircraft was softly suspended on elastic cords during the ground tests so that little external stiffness would be introduced into the airframe structure. Four eyebolts were connected to the airframe at the upper wing attachment screws, and the elastic cord was looped through the eyebolts and suspended from a single hook overhead, as shown in Figure 7. Two ropes were looped through the rear eyebolts and secured to stakes behind the aircraft to prevent twisting of the RPV during the engine run-up.

The accelerometer signals were first recorded with the engine off to measure the noise background. Then the engine was started, and data was measured with the engine operating at 500 rpm interval steps between 4600 and 7600 rpm. About 30 seconds of data acquisition was completed at each engine speed.

The first engine run-up was performed with the four isolators supporting the sensor payload plate, as shown in Figure 2. For the second ground test, the isolators were removed and replaced with four solid aluminum spacers so that the influence of the isolators could be evaluated.

Flight Testing

The three flights were performed with the launcher, ground control station, generators, instrumentation van, and recovery equipment located at a field site with an elevation of about 1550 m above mean sea level (MSL). The aircraft preparation was performed according to the normal Aquila procedures, with engine run-ups, aircraft checkouts using a portable "suitcase" tester, and ballasting for flight static stability.

The flights ranged up to about 20 km from the GCS, and the flight durations were 4440, 4500, and 3420 seconds (74, 75, and 57 minutes). The elevation angle of the line of sight from the GCS to the aircraft was confined below +0.183 radian (10.5 degrees) in order to remain in the pattern of the GCS high-gain antenna.

The way points in each flight plan were programmed prior to launch with way point locations, sequence, altitudes, and airspeeds. Manual control of the aircraft was made by the RPV operator in order to repeat or eliminate maneuvers as desired and to loiter during data tape changes.

Fig. 7. Ground test configuration.

Vibration and flight dynamics data were recorded for a wide range of flight conditions which covered the operating envelope of the Aquila. Measurements were also made with the aircraft on the launcher, both before and after engine start-up. This provided both a preflight check of the data link and background noise level measurements.

Straight-and-level flight, standard rate turn, and loiter data were recorded over a representative range of the following parameters: airspeeds (26 to 42 m/s), altitudes (1750 to 2270 m MSL, up to about 1000 m above the terrain), engine speeds (76 to 144 Hz, 4600 to 8600 rpm), altitude changes, angles between the aircraft flight path and the line of sight from the GCS to the RPV, atmospheric gust intensities, and distances from the GCS to the RPV. The loitering flight pattern was designed to provide a circular path over the ground with a diameter of one kilometer. Other maneuvers included launch, climbs, descents, double standard rate turns, roll jinking, pitch jinking, combined jinking, payload protector deployment, go-around, and recovery.

RESULTS

Analysis Procedures

Two data analysis procedures were employed: frequency domain spectral analysis for steady-state data, and time history plotting for transient data. The steady-state conditions included the ground suspension test, straight-and-level flight, turns, climbs, descents, loiter, and engine operation on the launcher. Jinking was analyzed using both techniques, and the other events were considered to be transients. Vertical gust velocity spectra were generated after correcting the gust vane data for rigid body motions of the aircraft.

Spectra were also taken for the instrumentation background noise to compare with the ground and flight data. For the ground suspension test this measurement was made with the engine off. For the flight test it was done with the aircraft on the launcher operating on ground power with the engine off and with external cooling air supplied to the aircraft transmitter.

The accelerometer spectral analyses were done on a constant bandwidth digital analyzer and the results plotted in two ranges: 20-300 Hz and 0.3-20 Hz. The analysis bandwidths were 0.125 and 1.25 Hz, respectively. Spectra from four 8 sec. time segments were averaged for each low frequency plot, and eight 0.8 sec. time segments were averaged for each high frequency plot. The low frequency range was not used for the ground test data because there were no excitation sources in this range, while the angular acceleration data taken in flight was not analyzed in the higher frequency range because of the limited frequency response of the angular transducers.

The primary scales used for the spectra plots were power spectral density (PSD) units of g^2/Hz and $(rad/sec^2)^2$/Hz. Because harmonic components were present in some of the linear acceleration plots, an amplitude scale in units of g's rms was also included where appropriate.

In the following sections the ground test results are considered first, then the flight test results. The flight test conditions were divided into two parts: those in which a payload sensor would operate, and those in which a sensor would have to survive when not operating.

Ground Test Data

Spectral analyses in the high frequency range were done for all the ground suspension test-RPM conditions for both the rubber isolator and rigid dummy isolator configurations. Table 2 lists the test conditions, and Figures 8-10 show typical spectral plots for both isolator configurations.

The ground test spectra were characterized by a broad peak centered around 35 Hz and narrow peaks at the engine rotation frequency and its first harmonic. The 35 Hz peak varied little with RPM but had a different shape and, in most cases, a lower amplitude in the dummy isolator case compared with the rubber isolator case. A number of sources could have contributed to this peak including resonances in the fuselage structure, resonant motion of the payload on its isolators, and resonant motion of the engine on its isolators. Resonant frequencies calculated for the last two cases fell within the range covered by the peak. The higher response in the rubber isolator case was

TABLE 2

GROUND SUSPENSION TEST CONDITIONS

TEST CONDITION NO.	ENGINE SPEED	
	RUBBER ISOLATORS RPM (Hz)	RIGID, DUMMY ISOLATORS RPM (Hz)
1	4620 (77)	4530 (76)
2	4920 (82)	5100 (85)
3	5460 (91)	5490 (92)
4	6030 (101)	6060 (101)
5	6420 (107)	6510 (109)
6	7050 (118)	7050 (118)
7	7650 (128)	7680 (128)

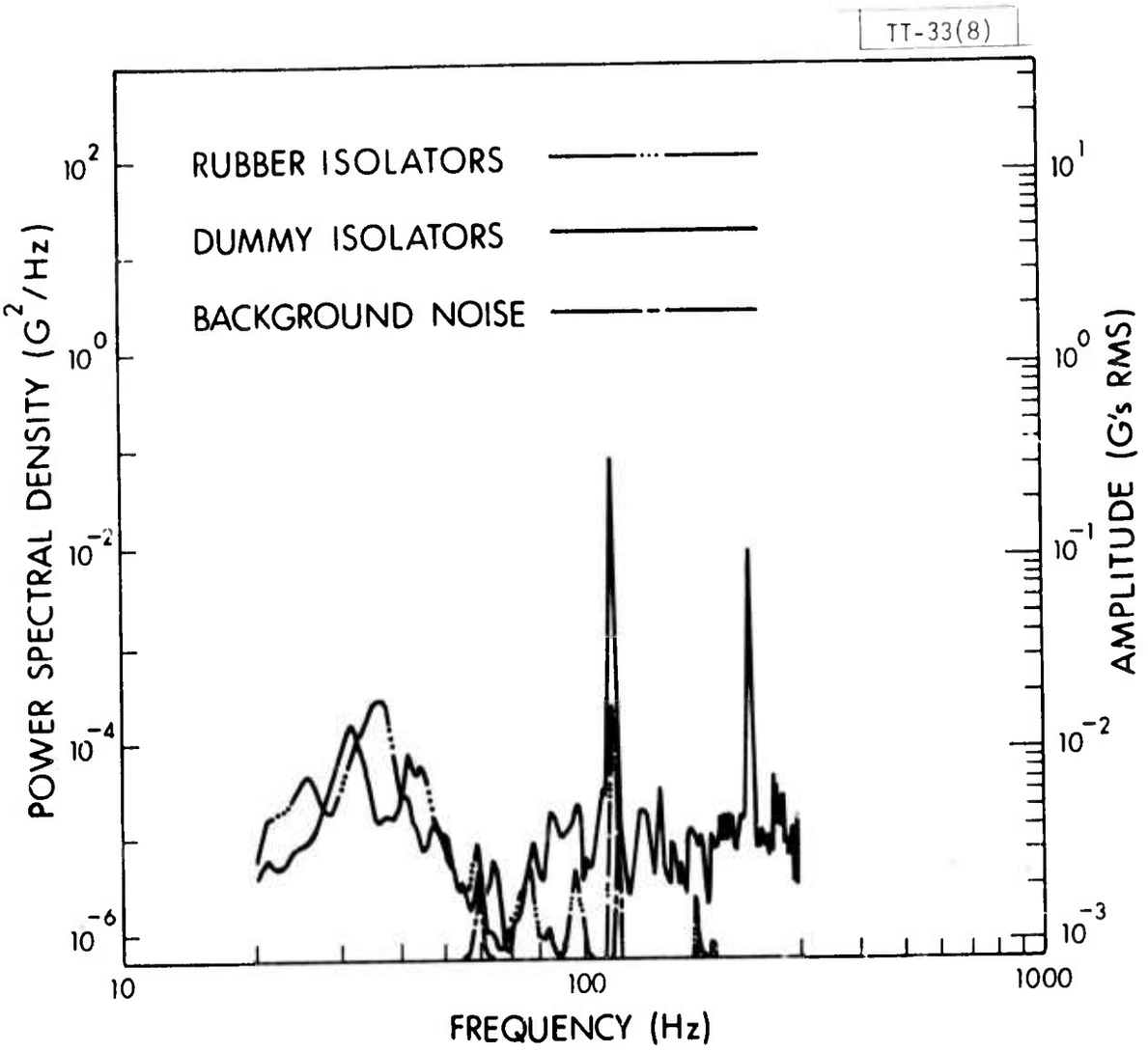

Fig. 8. Ground suspension test example spectra — fore-and-aft acceleration.

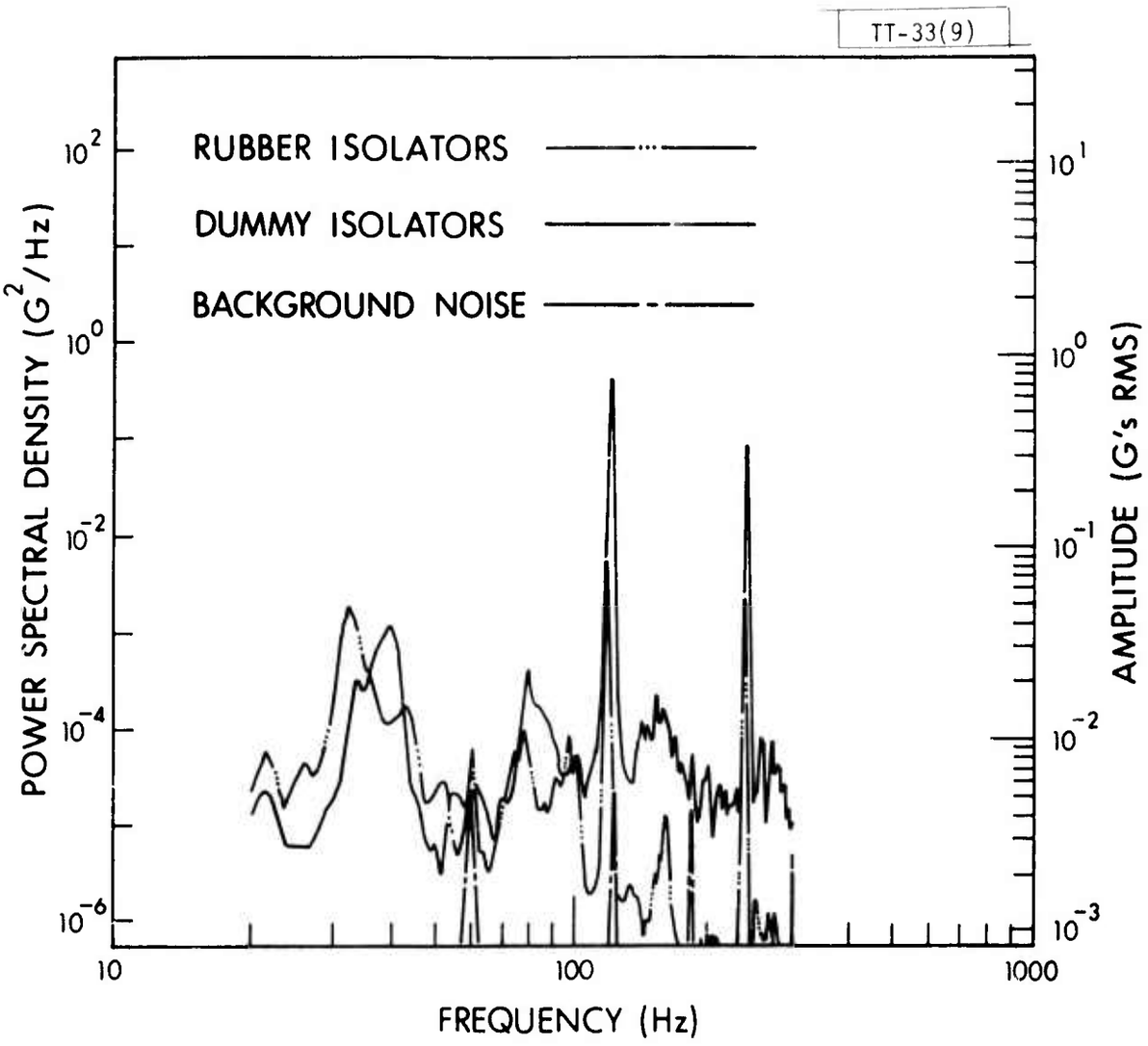

Fig. 9. Ground suspension test example spectra — lateral acceleration.

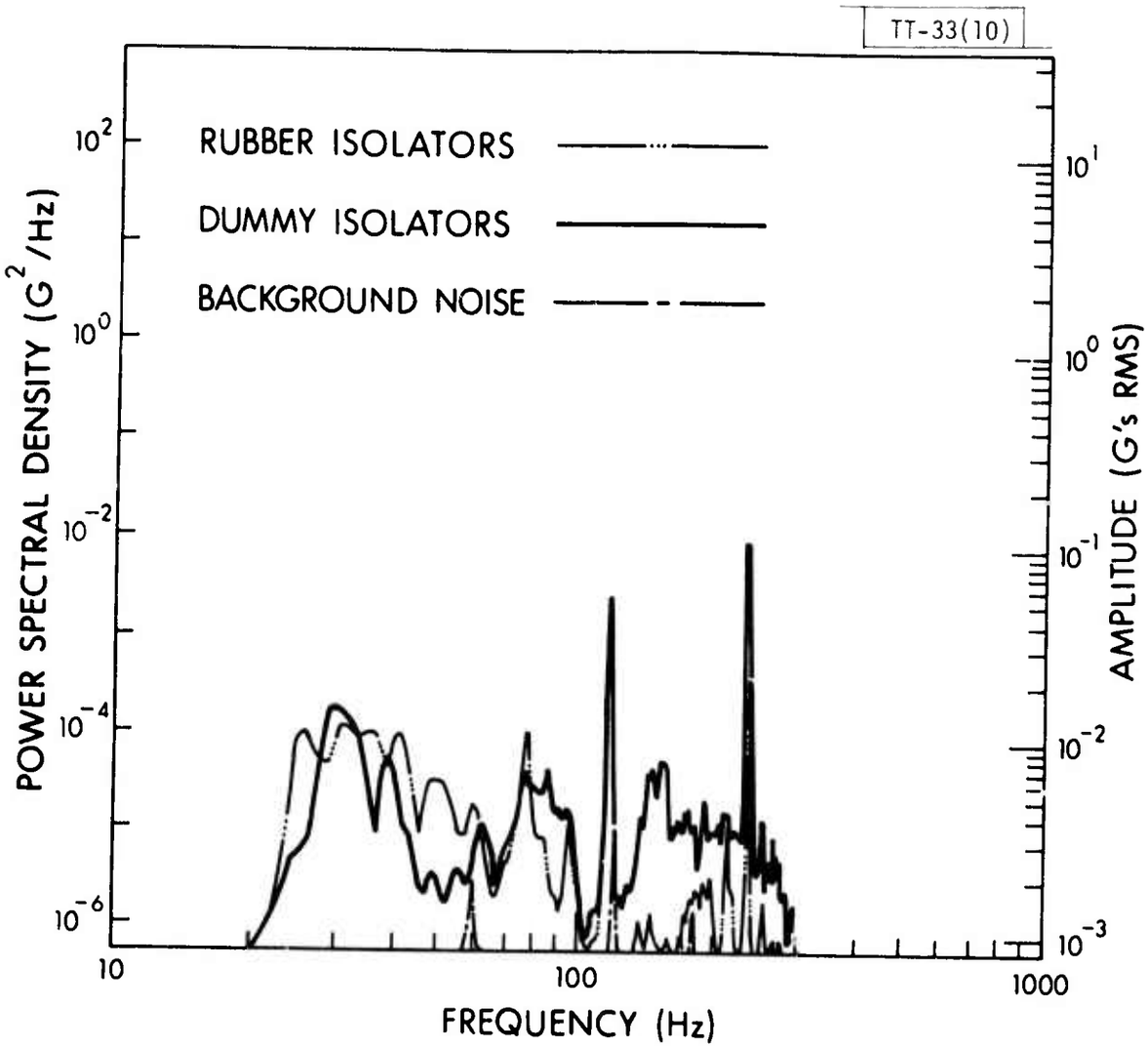

Fig. 10. Ground suspension test example spectra – vertical acceleration.

expected since the isolators amplify the vibration levels near their resonant frequencies. The payload itself was essentially rigid in the frequency range considered here, so local resonances of the payload should not have contributed to the response peak. In general the peaks at the engine rotation frequencies were lower in the rubber isolator case. This was expected since the isolators attenuate inputs above the payload-isolator natural frequency.

The response near 35 Hz was probably a combination of random and harmonic components, while the engine rotation produced pure harmonic components. The PSD units should be used for the random components and the amplitude units for the harmonic components.

Operational Flight Conditions

Representative sections of the flight data were chosen for analysis, and the flight conditions are summarized in Table 3. The operational flight conditions were chosen from this list, and Figure 11 shows a typical spectral plot in the high frequency range. The spectra were similar in shape to the spectra for the ground test rubber isolator configuration with a characteristic broad peak centered around 35 Hz and single frequency peaks between 77 and 145 Hz. The latter corresponded to the engine rotation speeds of 4620-8700 RPM seen in the flight data. A second grouping of peaks occurred between 154 and 290 Hz at the 1st harmonics of the engine rotation frequencies. At the primary engine frequencies the peaks were highest at the low RPM and high RPM ranges and lower in the middle RPM range.

In the 20-300 Hz range the spectra had the same general shape for all the flight conditions and measurement directions. There was no significant difference between straight-and-level and turning flight, and no trends could be detected with changes in airspeed or flight direction.

In the low frequency range, 0.3-20 Hz, the PSD levels were different for each measurement axis, and an example plot for each component is shown in Figures 12-17. In the X and Y directions the linear acceleration levels were barely above the background noise. In contrast to the spectra levels in the higher frequency range, the low frequency spectra levels varied with gust velocity, airspeed, and maneuvers, but they were not correleated with RPM changes.

TABLE 3

FLIGHT CONDITIONS

EVENT NO.	FLIGHT NO.	FLIGHT CONDITION	ENGINE SPEED RPM (Hz)	AIRSPEED km/hr (m/s)	ALTITUDE m, MSL	VERT. GUST VELOCITY m/s rms
1	2	Engine Running on Launcher	6600 (110)		1550	
2	2	Straight and Level	4575 (76)	97 (27)	2270	2.72
3	2	Straight and Level	8325 (139)	135 (38)	1750	1.22
4	2	Straight and Level	8625 (144)	150 (42)	1990	1.90
5	2	Loiter-Right Hand	7950 (133)	92 (26)	2110	2.31
6	2	Double Standard Rate Turn-Right	8175 (136)	102 (28)	2040	
7	2	Double Standard Rate Turn-Left	8100 (135)	100 (28)	2022	
8	2	Roll Mode Jink	8025 (134)	83-107 (23-30)	2080	
9	2	Pitch Mode Jink	8325 (139)	113-193 (31-54)	1850-1950	
10	2	Combined Mode Jink	8025 (134)	90-174 (25-48)	1950-2065	
11	2	Straight and Level-Payload Protector Deployed	7600 (127)	94 (26)	1600	
12	3	Engine Running on Launcher	4620 (77)		1550	
13	3	Straight and Level	5100 (85)	95 (26)	1650	1.26
14	3	Straight and Level	5850 (98)	115 (32)	2220	2.38
15	3	Straight and Level	7500 (125)	100 (28)	1800	1.23
16	3	Straight and Level	7575 (126)	92 (26)	2180	0.89
17	3	Straight and Level	7650 (128)	112 (31)	2050	1.36
18	3	Straight and Level	7750 (129)	135 (38)	2050	1.39
19	3	Straight and Level	7875 (131)	135 (38)	2250	1.82

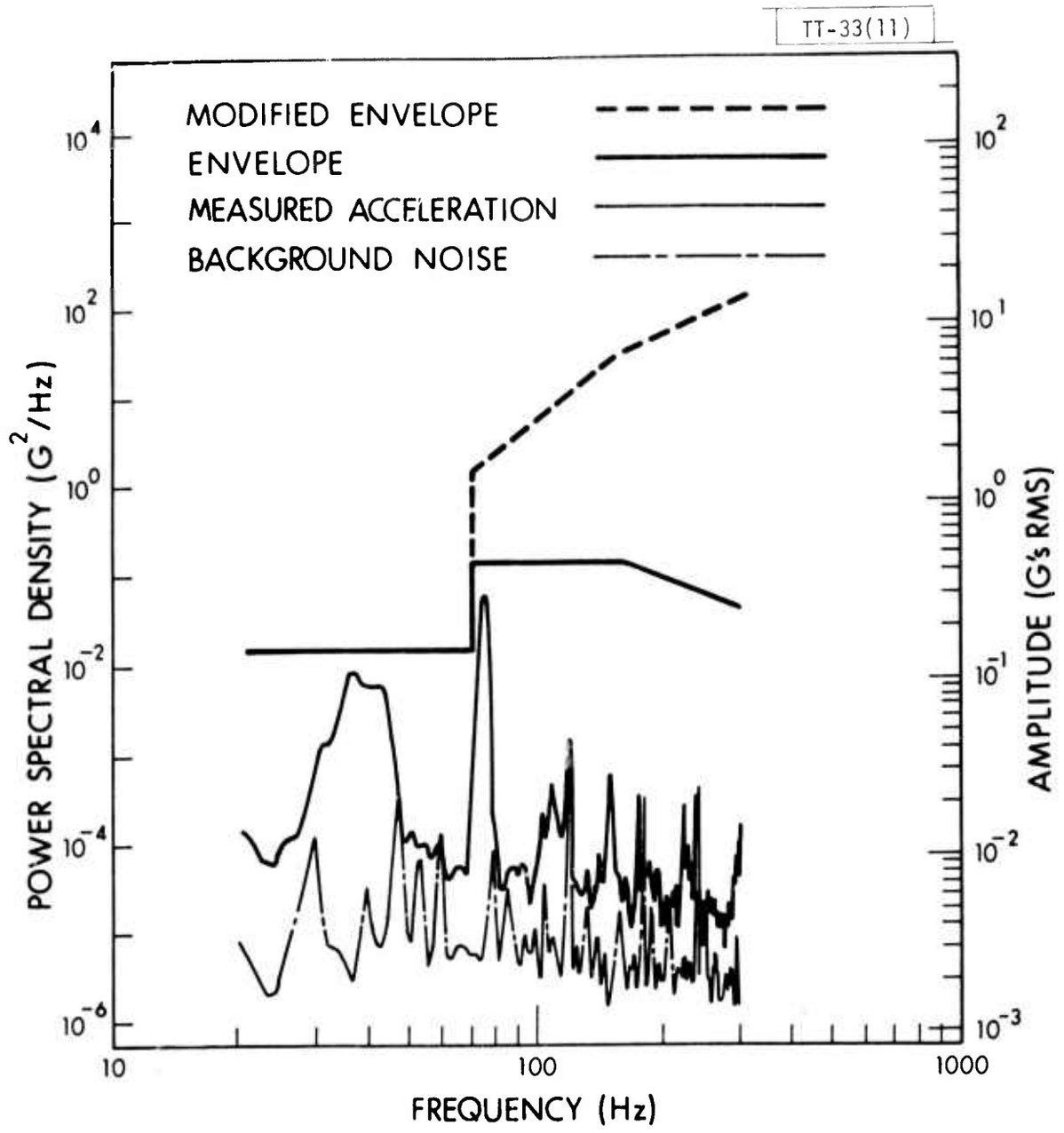

Fig. 11. Flight test example spectrum and envelopes — linear acceleration — high frequency range.

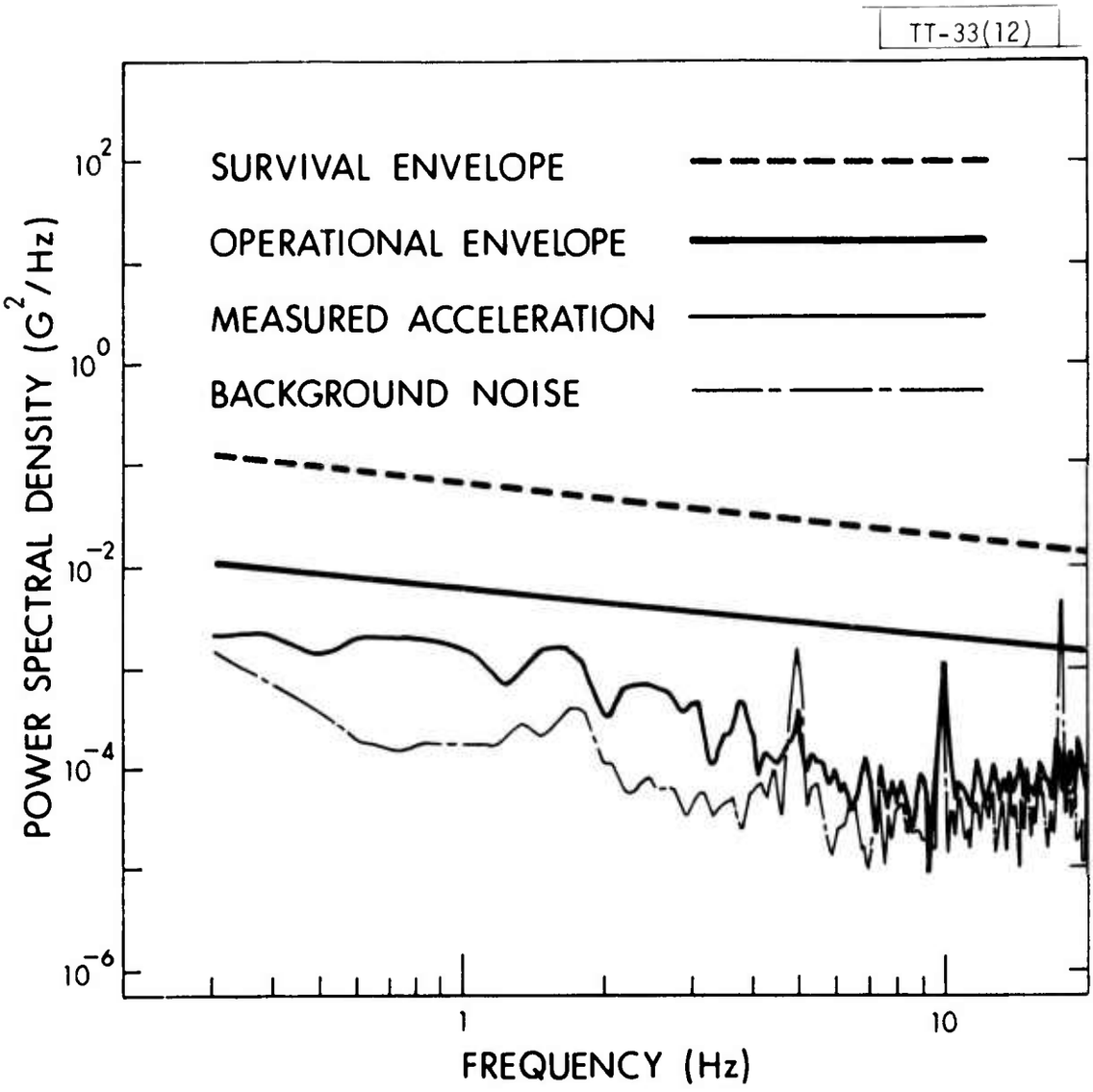

Fig. 12. Flight test example spectrum and envelopes — fore-and-aft acceleration — low frequency range.

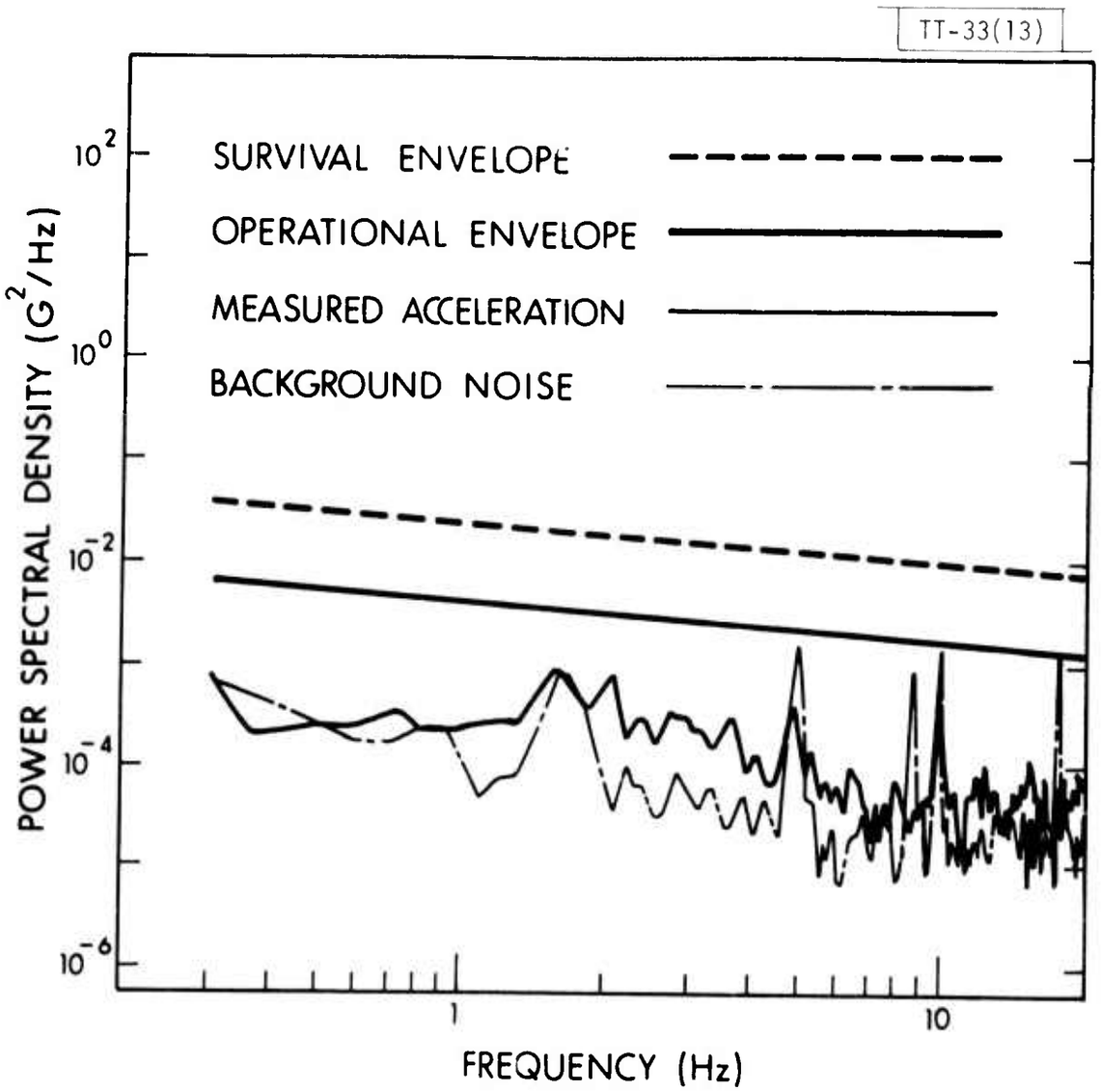

Fig. 13. Flight test example spectrum and envelopes — lateral acceleration — low frequency range.

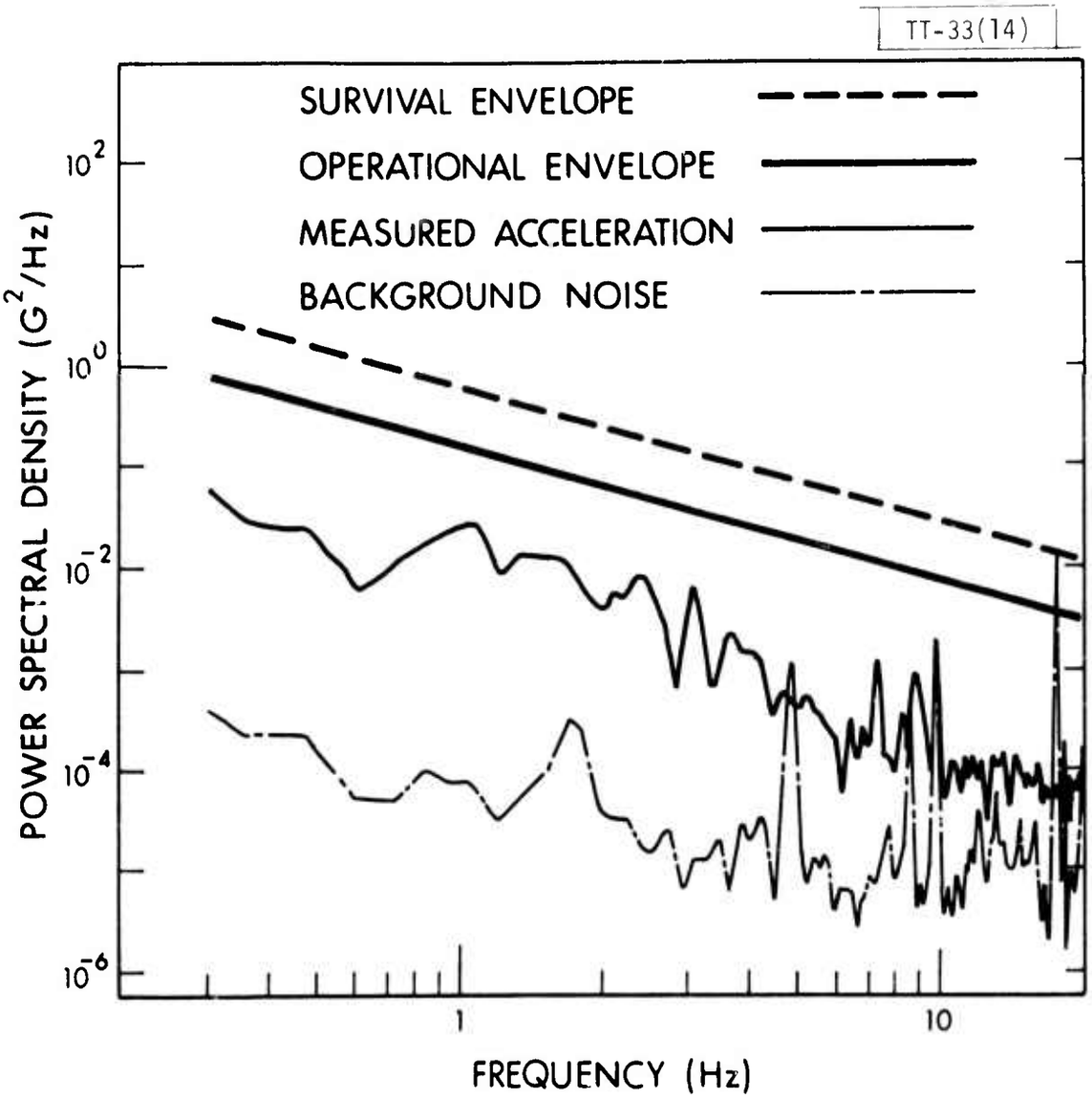

Fig. 14. Flight test example spectrum and envelopes — vertical acceleration — low frequency range.

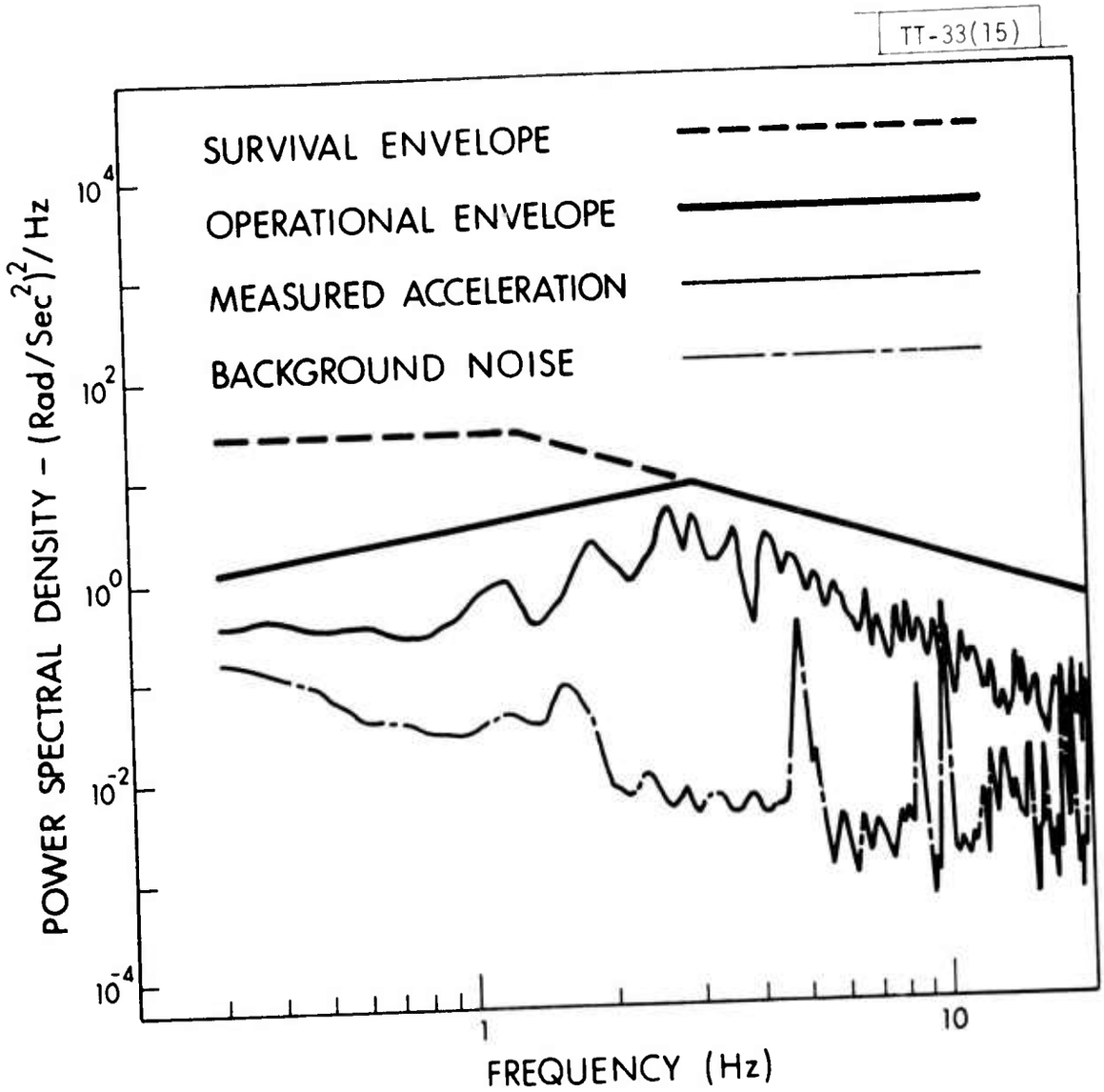

Fig. 15. Flight test example spectrum and envelope — roll acceleration.

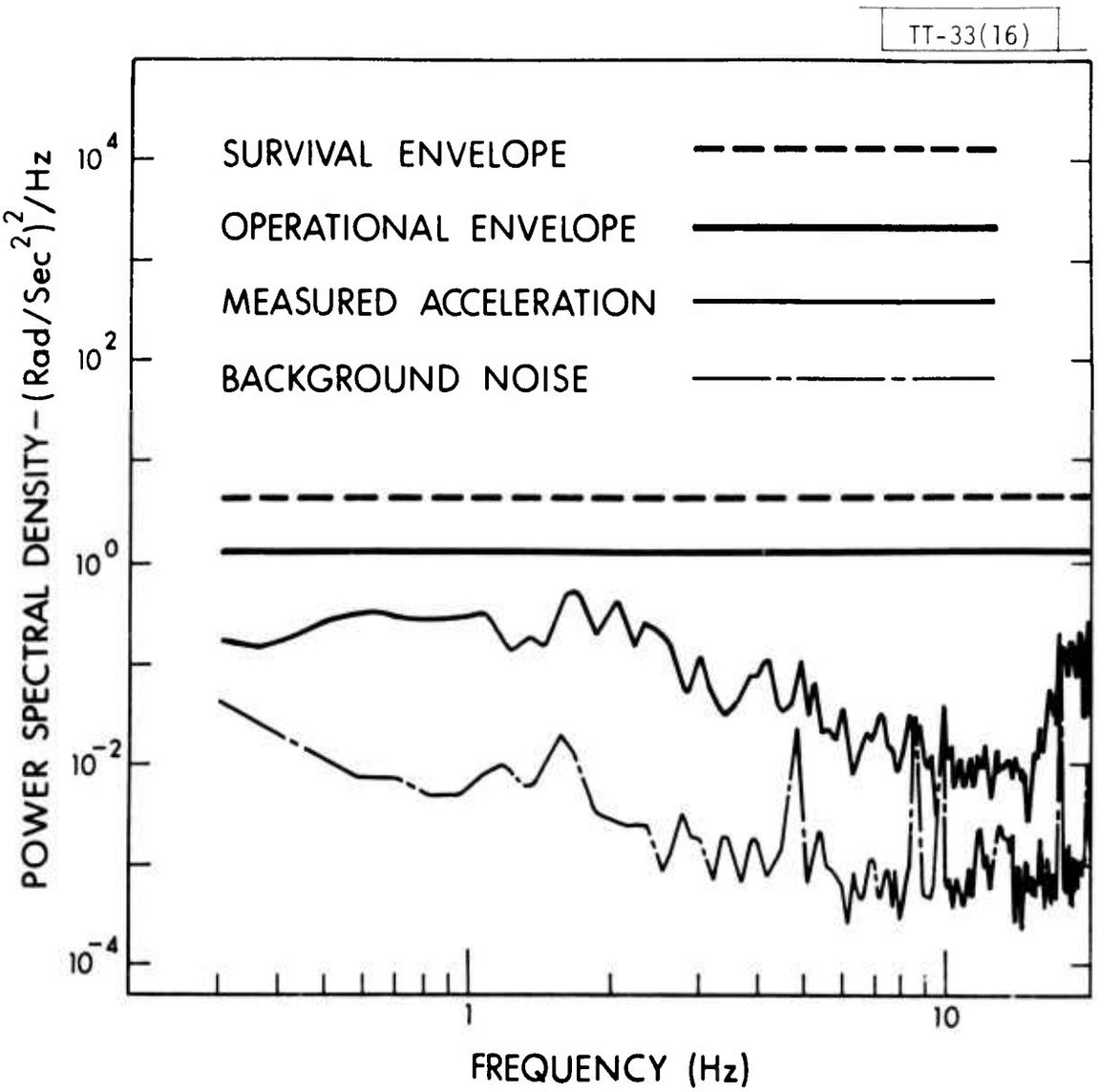

Fig. 16. Flight test example spectrum and envelope – pitch acceleration.

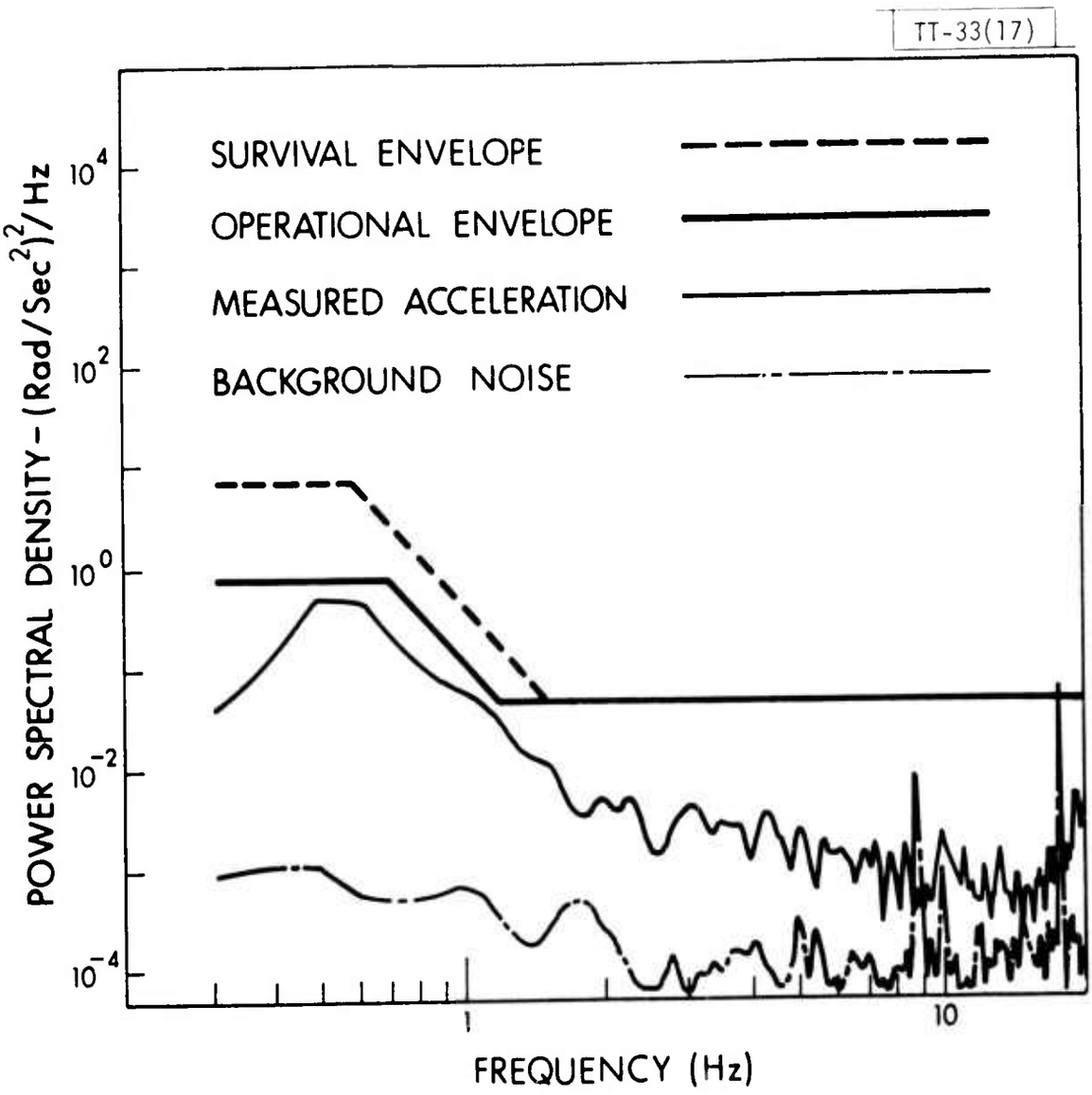

Fig. 17. Flight test example spectrum and envelope — yaw acceleration.

The yaw spectra levels showed a significant increase in response around 0.6 Hz for all flight conditions. This was caused by a "weathervane" yaw mode, and calculations using wind tunnel measurements[2] of yawing moment due to sideslip (C_{n_β}) and the airspeed and local air density predicted a yaw mode in the 0.4-0.8 Hz range. Similar yaw motions were observed in previous experiments with a different mini-RPV[3].

To provide a specification for the sensor operational environment, the spectra for the operational flight conditions were enveloped. For this operation the spectra were divided into three regions: 0.3-20 Hz, where the aircraft responded rigidly to aerodynamic inputs and all responses were considered random; 20-70 Hz, where the payload isolators amplified the levels and the responses were considered a combination of random and harmonic; and 70-300 Hz, where the engine excitation was dominant and all responses were considered harmonic.

One spectrum envelope covering 20-300 Hz was produced for all three linear acceleration spectra since they all had similar shapes, and it is shown with the example spectrum in Figure 11. The portion of the envelope between 70 and 300 Hz is for harmonic components only, and the g's rms scale applies. The portion between 20 and 70 Hz covers both random and harmonic components, and both scales apply. In the low frequency range a PSD envelope was produced for each measurement axis, and these are shown with the example spectra in Figures 12-17.

To eliminate the effects of the payload isolators from the previous results, the spectra envelopes were modified using the characteristics of the isolators and the results from the ground suspension test. Below the natural frequencies of the payload-isolator combination the vibration levels were not changed by the isolators, so the envelopes were not modified below 20 Hz. Between 20 and 70 Hz, where the resonances of the payload-isolator combination occurred, the isolators amplified the vibration levels. Because of the many resonant modes of the payload-isolator combination and the difficulty in identifying them in the flight data, the envelope was also not modified in the 20-70 Hz region. This ensured a conservative result.

Above 70 Hz the isolators attenuated the vibration levels at about 12 dB/octave. However, before this factor was applied, the results from the two ground suspension test configurations were compared to determine the maximum difference between the rubber isolator and dummy isolator spectral levels at 70 Hz. This factor was 3, and it was applied to the amplitude spectrum envelope at 70 Hz. The 12 dB/octave factor was then applied starting at 70 Hz with the results shown by a dashed line in Figure 11. This provided a specification which eliminated the effect of the isolators but which was valid only for payloads with approximately the same weight as that used for the flight test.

Survival Flight Conditions

Envelopes were also produced for those survival conditions which could be analyzed spectrally. These included all jinking modes, engine operation on the launcher, double standard rate turns, and a large oscillation at 1.6 Hz in the X and Y acceleration data that appeared after the payload protector deployment (event number 11 in Table 3). All these events produced spectra below the operational spectra envelopes except for the jinking and 1.6 Hz oscillations which produced higher low frequency spectra. Envelopes for the survival conditions are shown in Figures 12-17.

Jinking was also analyzed as a transient event because some of the dynamic responses of the aircraft were too slow to show up in the low frequency spectra. The Z accelerometer had a large response in the pitch and combined jinking modes with maximum responses of 4.7 g P-P at an average frequency of 0.17 Hz. The "weathervane" mode showed up strongly on the yaw accelerometer with the largest responses during the roll and combined jink modes. Maximum responses were about 4.5 rad/sec^2 P-P at an average frequency of about 0.6 Hz. Figure 18 shows time histories for all six axes for the combined jink mode. The time histories were low-pass filtered at 20 Hz before plotting.

Launch and recovery accelerations were not obtained because the levels were beyond the range of the instrumentation. Estimated limits on these accelerations are in the Aquila RPV technical manual.[4]

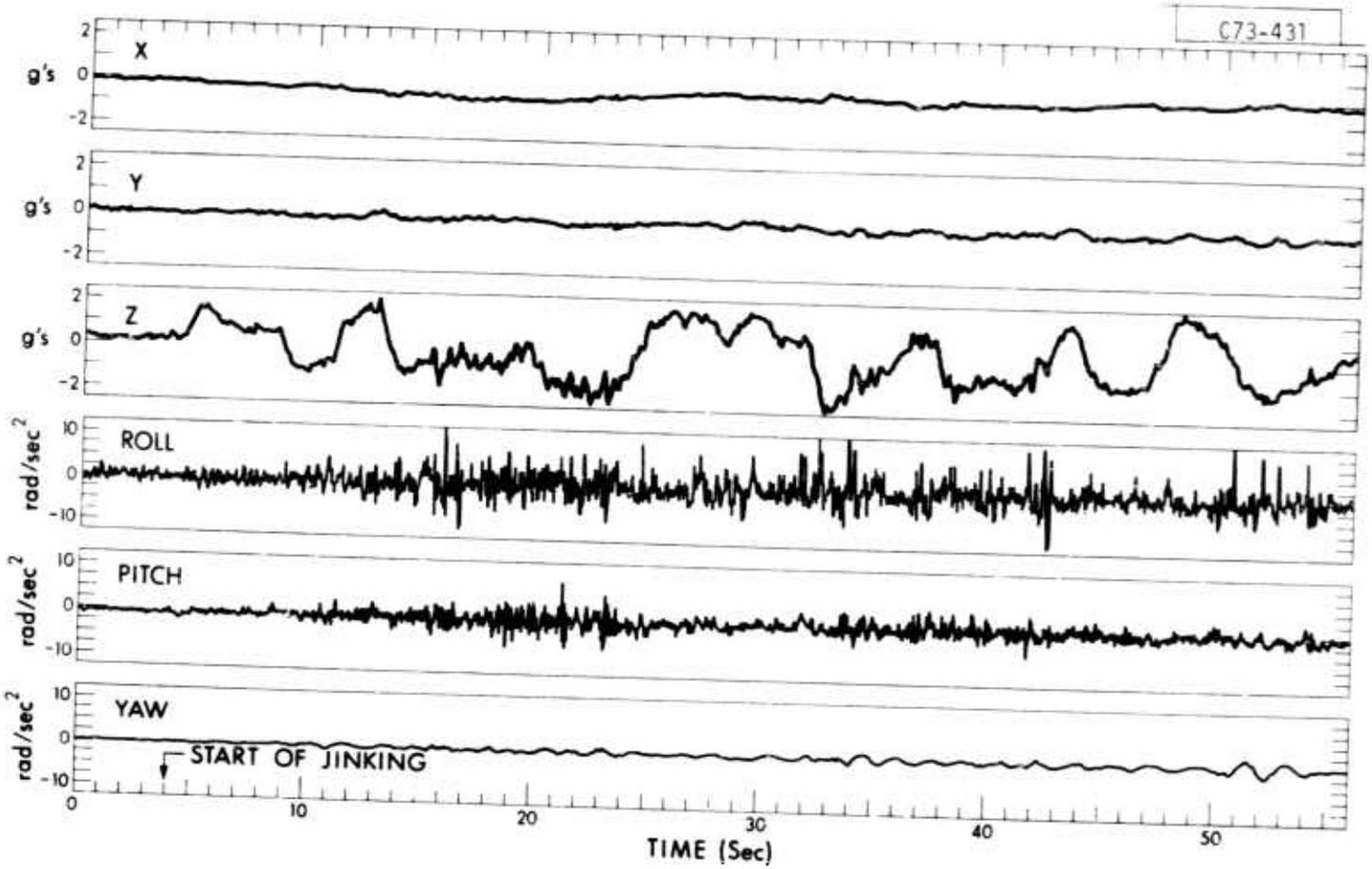

Fig. 18. Combined jinking acceleration time histories.

Transient response to turn initiation was studied in the double standard rate turn data. This was a turn with twice the 3^{o}/sec standard turn rate. In one of the data samples the turn initiation produced a pulse of about 9 rad/sec^2 in the roll acceleration but was not detectable on any of the other channels. This response was less than the steady-state levels seen during other turns, so it was not a significant transient event.

Rapid engine speed changes were studied as a possible source of transient responses, but the engine speed changes were slow enough to prevent any such response.

Deployment of the payload protector produced a shock response which is shown in time history form in Figure 19. The pitch axis had the largest angular acceleration response, and the signal was clipped because it was beyond the range of the accelerometer. Since the measurement was made on the payload plate, it necessarily includes the filtering effect of the payload isolators.

An aborted landing approach, or "go-around," occurred during the third flight, and this provided an opportunity to see the effects of a maximum performance maneuver and the dynamic loading from elevon deflections. Go-around time histories, low-pass filtered at 20 Hz, are shown in Figure 20. About 8 seconds before the go-around command the "weathervane" yaw mode and accompanying high roll accelerations were excited to a higher level than at any other time in flight. The maximum yaw response was 5.5 rad/sec^2 P-P at an average frequency of 0.6 Hz. No specific cause was found for these high amplitudes. Shortly after the go-around decision a large spike occurred in the pitch acceleration, probably due to elevon deflection. The weathervane response died out immediately after this spike.

Vertical Gust Environment

The vertical gust velocity components of the atmospheric turbulence through which the aircraft flew were assumed to follow the spectra attributed to von Karman (Reference 5), which can be written as:

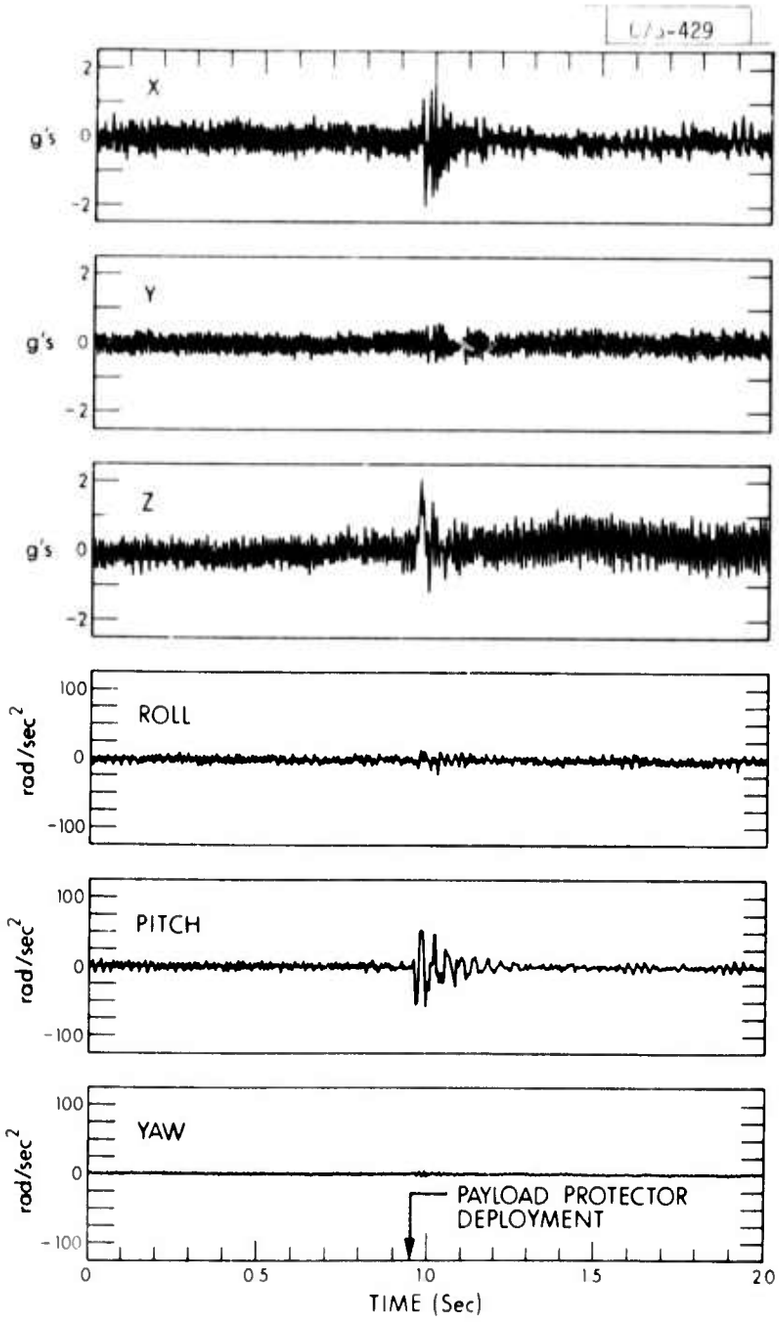

Fig. 19. Payload protector deployment acceleration time histories.

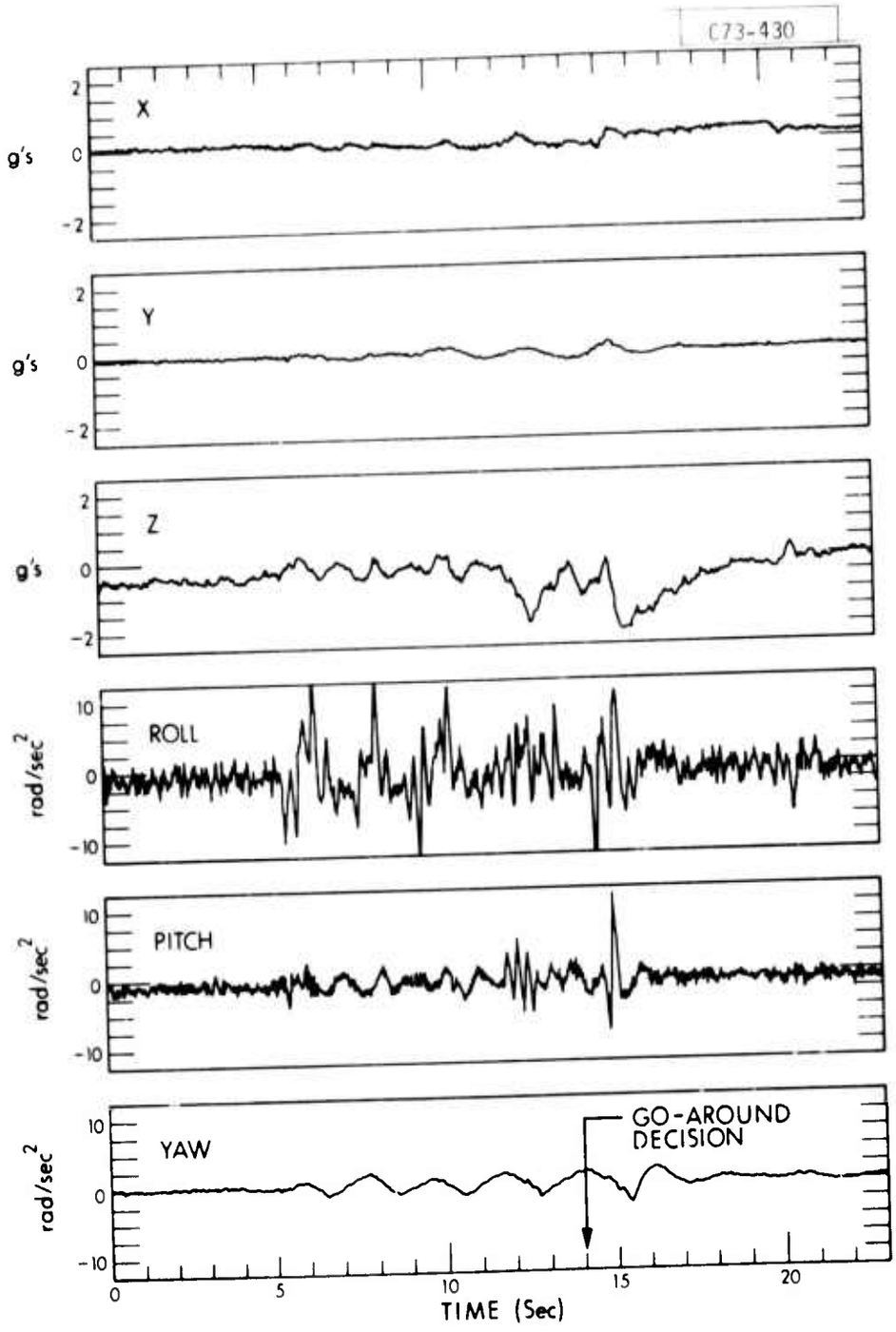

Fig. 20. Go-around acceleration time histories.

$$PSD_w = \frac{2\sigma_w^2 L}{V} \frac{\left[1 + 189\left(\frac{fL}{V}\right)^2\right]}{\left[1 + 70.8\left(\frac{fL}{V}\right)^2\right]^{11/6}} .$$

The symbols are defined as follows: PSD_w = power spectral density of the vertical gust velocity in $(m^2/s^2)/Hz$, σ_w = rms vertical gust velocity in m/s, L = scale length of vertical gust velocity in m, V = aircraft forward airspeed in m/s, and f = frequency in Hz. For sufficiently large values of fL/V, the spectra can be expressed as $PSD_w \approx (0.153)\ \sigma_w^2\ V^{2/3}\ L^{-2/3}\ f^{-5/3}$, which approximates the above equation within two percent for (fL/V) > 1.

For the analyzed flight patterns representative of sensor operation, the rms amplitudes and spectra of the vertical gust velocities were measured for frequencies between 0.375 and 50 Hz. Spectra from four 8 second time segments were averaged for each spectral curve, and the analysis bandwidth was .125 Hz. The corrections to the gust vane motions to account for vertical and pitch angular motions of the aircraft were included, although their influence was not important for frequencies above about 3 Hz.

The overall rms amplitudes of the vertical gust velocities were calculated according to the equation in Reference 6 which relates the overall rms amplitudes for the von Karman spectrum to rms amplitudes measured over a discrete frequency range:

$$\sigma_w^2 = (4.35)\ \frac{\sigma_1^2\ L^{2/3}\ f_a^{2/3}\ f_b^{2/3}}{V^{2/3}\left(f_b^{2/3} - f_a^{2/3}\right)},$$

where σ_w is the overall rms value, σ_1 is the rms value over the measured frequency range, and f_a and f_b are the lower and upper limits of the measured frequency range in Hz. To calculate the overall vertical gust velocities, the scale length was assumed to equal about 150 m, a representative value for atmospheric turbulence given in Reference 5.

The vertical gust amplitudes for eleven flight paths representative of flight during sensor operation are listed in Table 3. The listed range of gust velocities corresponded to cumulative probabilities between 0.013 and 0.57 according to representative gust severity probability curves in Reference 5. The probability range means that for a representative sample of vertical gusts in the atmosphere, about fifty-seven percent of gusts have intensities larger than the smallest of the eleven samples, and about ninety-nine percent of gusts have intensities smaller than the largest of the eleven samples.

For each of the eleven measured rms gust intensity values, a von Karman spectrum was constructed and compared to the measured spectrum. All eleven spectra were found to agree with the von Karman spectra relatively well, with no particular resonance effects in the range of gust vane natural frequencies, 9 to 15 Hz. One such comparison is shown in Figure 21. It should be pointed out that the contributions of the spectrum between 9 and 50 Hz to the calculated overall rms gust intensities would be less than five percent for the von Karman spectrum.

CONCLUSIONS

The flight vibration environment for the isolated payload was a combination of random and harmonic components covering a wide frequency range. Below 20 Hz the aircraft was essentially rigid, and it was excited by random aerodynamic inputs. The most significant response in this range was a "weathervane" yaw mode at about 0.6 Hz. From 20 to 70 Hz there was an increase in response due to resonances of the payload on its isolators, with contributions from the aircraft structure and possibly the engine on its isolators. These responses had the combined characteristics of both random and harmonic components. Above 70 Hz, discrete frequency components at the engine rotation frequency and its first harmonic were the dominant response. The engine frequency ranges for the flight conditions studied were 77-145 Hz for the primary rotation frequency and 154-290 Hz for the harmonic.

The vertical gust velocities measured in flight covered a wide range with maximum intensities more severe than 99 percent of gusts in clear air, according

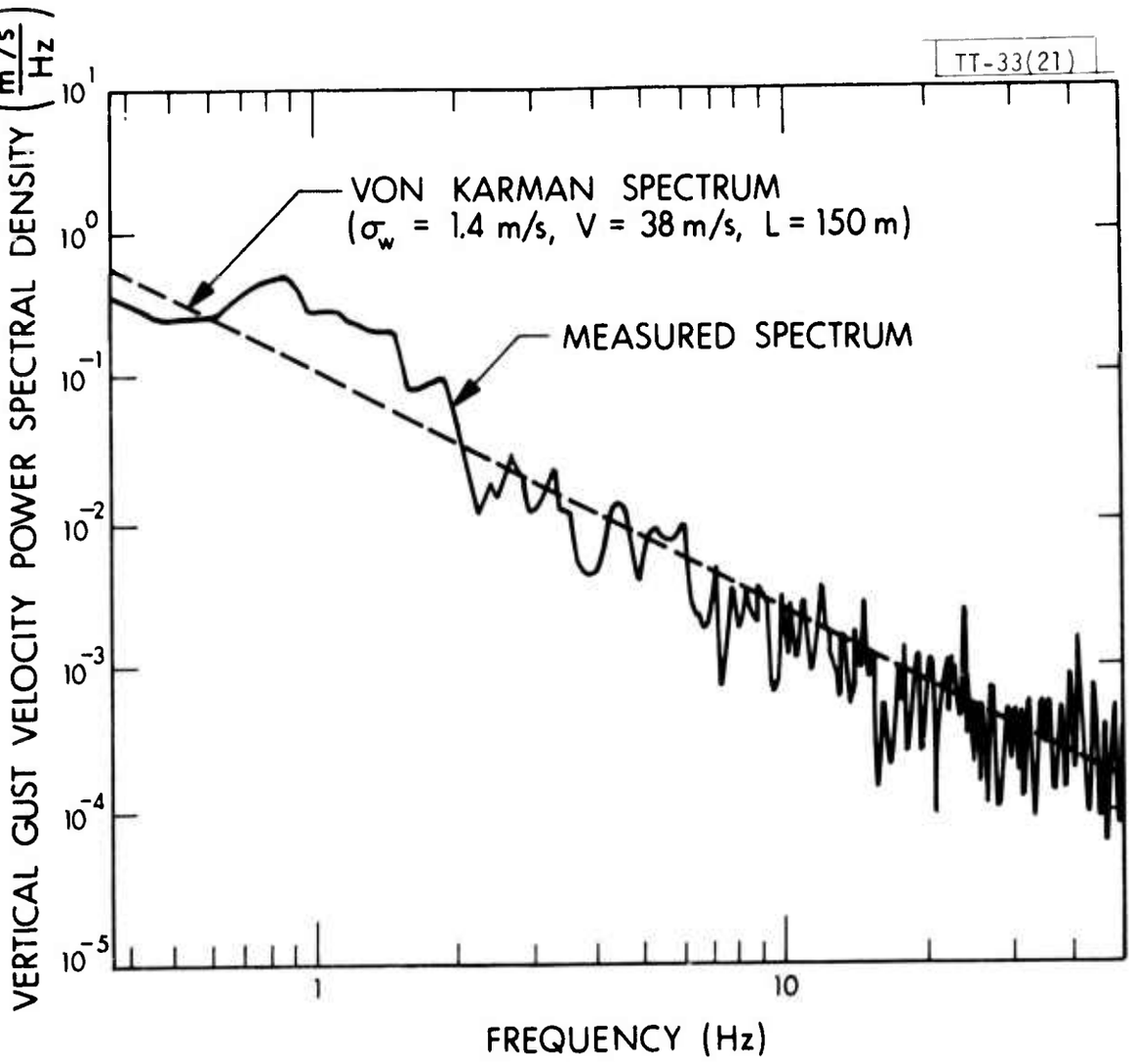

Fig. 21. Sample vertical gust velocity spectrum.

to representative probability curves[5]. The measured gust velocity spectra agreed with the von Karman formulation describing atmospheric turbulence.

Acceleration spectra for two types of flight conditions were enveloped: those in which a sensor would have to operate; and those in which a sensor might not operate but would have to survive. The envelopes are shown in Figures 11-17. There is only one envelope in the 20-300 Hz range because the spectra were similar for all three measurement axes. To remove the effects of the payload isolators, the envelopes were modified using the results of the ground suspension test. The correction applied only above 70 Hz, and it increased the envelope level significantly as shown in Figure 11. The envelopes are valid only for payloads with approximately the same weight as that used for the flight test.

Several of the transient events were significant survival conditions. The pitch and combined jinking modes produced a sinusoidal vertical load of 4.7 g P-P at an average frequency of about 0.17 Hz, and deployment of the payload protector produced a shock-type response which is illustrated in Figure 19.

REFERENCES

1. J. T. Karam, Jr., "Dynamic Behavior of Angle of Attack Vane Assemblies," AIAA J. 12, 190 (1975). Also, Air Force Institute of Technology Report, TR-74-8 (December 1974).

2. "RPV System Test Report, CDRL A00D, Part 4, Aerodynamics," LMSC-L028081, Lockheed Missiles and Space Co., Sunnyvale, CA (May 1977).

3. P. O. Jarvinen and C. F. Bruce, "Mini-RPV Flight Dynamics Measurements," AIAA Guidance and Control Conference, San Diego, CA (August 1976).

4. "Technical Manual for Aquila RPV System Technology Demonstrator, Vol. 1, System Description," LMSC-D056906, Lockheed Missiles and Space Co., Sunnyvale, CA (10 August 1977).

5. J. C. Houbolt, "Atmospheric Turbulence," AIAA J. 11, 421 (1973).

6. J. C. Houbolt, R. Steiner, and K. G., Pratt, "Dynamic Response of Airplanes to Atmospheric Turbulence Including Flight Data on Input and Response," NASA TR R-199, NASA Langley (June 1964).

UNCLASSIFIED

SECURITY CLASSIFICATION OF THIS PAGE *(When Data Entered)*

REPORT DOCUMENTATION PAGE

READ INSTRUCTIONS BEFORE COMPLETING FORM

1. REPORT NUMBER: ESD-TR-78-367	2. GOVT ACCESSION NO.
3. RECIPIENT'S CATALOG NUMBER	
4. TITLE *(and Subtitle)*: XMQM-105 (Aquila) Mini-RPV Vibration and Flight Dynamics Measurements	5. TYPE OF REPORT & PERIOD COVERED: Project Report
	6. PERFORMING ORG. REPORT NUMBER: Project Report TT-33
7. AUTHOR(s): Charles F. Bruce and William R. Davis	8. CONTRACT OR GRANT NUMBER(s): F19628-78-C-0002
9. PERFORMING ORGANIZATION NAME AND ADDRESS: Lincoln Laboratory, M.I.T. P.O. Box 73 Lexington, MA 02173	10. PROGRAM ELEMENT, PROJECT, TASK AREA & WORK UNIT NUMBERS: ARPA Order-2752 Program Element No. 62702E Project Code 9G10
11. CONTROLLING OFFICE NAME AND ADDRESS: Defense Advanced Research Projects Agency 1400 Wilson Boulevard Arlington, VA 22209	12. REPORT DATE: 8 December 1978 13. NUMBER OF PAGES: 50
14. MONITORING AGENCY NAME & ADDRESS *(if different from Controlling Office)*: Electronic Systems Division Hanscom AFB Bedford, MA 01731	15. SECURITY CLASS. *(of this report)*: Unclassified 15a. DECLASSIFICATION DOWNGRADING SCHEDULE

16. DISTRIBUTION STATEMENT *(of this Report)*

Distribution limited to U. S. Government agencies only; test and evaluation; 3 January 1979. Other requests for this document must be referred to ESD/TOFL (Lincoln Laboratory), Hanscom AFB, MA 01731.

17. DISTRIBUTION STATEMENT *(of the abstract entered in Block 20, if different from Report)*

18. SUPPLEMENTARY NOTES

None

19. KEY WORDS *(Continue on reverse side if necessary and identify by block number)*

XMQM-105 (Aquila)	flight dynamics
mini-rpv	vertical gust velocity
vibration	sensor payload vibration isolators

20. ABSTRACT *(Continue on reverse side if necessary and identify by block number)*

Vibration, flight dynamics, and vertical gust velocity measurements were performed for the XMQM-105 (Aquila) miniature remotely piloted vehicle. The effects of operating the engine over its range of speeds and the influence of the sensor payload vibration isolators were evaluated using ground test vibration data. The amplitudes and spectra of vibration and flight dynamic accelerations were analyzed for test flights in operational-type patterns. One significant flight dynamic motion observed was a yaw oscillation at a frequency of about 0.6 Hz. To provide a specification for the sensor payload vibration environment, the acceleration spectra were enveloped; and the envelopes were modified to remove the effects of the payload isolators. Acceleration time histories were examined for flight maneuvers and transient events, and the peak loads for these conditions were measured.

DD FORM 1 JAN 73 1473 EDITION OF 1 NOV 65 IS OBSOLETE

UNCLASSIFIED

SECURITY CLASSIFICATION OF THIS PAGE *(When Data Entered)*